Tectonophysics 799 (2021) 228688

Contents lists available at ScienceDirect

Tectonophysics

journal homepage: www.elsevier.com/locate/tecto

# Tectonic regimes and stress patterns in the Vrancea Seismic Zone: Insights into intermediate-depth earthquake nests in locked collisional settings

Laura Petrescu [a,*], Felix Borleanu [a], Mircea Radulian [a,b], Alik Ismail-Zadeh [c,d], Liviu Maţenco [e]

[a] National Institute for Earth Physics, Bucharest, Romania
[b] Academy of Romanian Scientists, AcadCtists, Splaiul Independentei, 54, 050094 Bucharest, Romania
[c] Karlsruhe Institute of Technology, AGW, Karlsruhe, Germany
[d] Russian Academy of Sciences, IEPTMG, Moscow, Russia
[e] Utrecht University, Utrecht, Netherlands

ARTICLE INFO

*Keywords:*
Seismic nest
Focal mechanisms
Stress inversion
Crust-mantle coupling

ABSTRACT

Earthquake nests are anomalous clusters of seismicity located far from active collisional systems in intraplate, locked suture zones, or the deep part of relic subducted slabs, challenging classic earthquake generation mechanism theories. The Vrancea Seismic Zone in Romania is such an upper-mantle seismic nest located in the SE Carpathians, releasing the largest strain in continental Europe. To better understand earthquake generation and the relationship with lithospheric deformation, we estimate earthquake source parameters in Vrancea and surrounding regions between 2014 and 2020, and determine the stress field via focal mechanism inversion and unsupervised machine learning. In the crustal domain, maximum horizontal stress is in agreement with surface fault kinematics and GPS-derived S-SE trending horizontal plate velocities relative to Eurasia, implying that tectonic stress is vertically coherent on a crustal scale. The stress regime changes from transpression beneath the orogen to transtension towards the foreland where movement is accommodated along major crustal faults, and tension further away from the epicentre, in the Moesian Platform and the North Dobrogea Orogen. Inside the seismogenic body vertical tension and an overall compressive regime dominates, implying that vertical elongation may be the driving mechanism for brittle failure and that stress is transmitted along the sinking slab to the surface. However, the retrieved stress ratios are low: ~0.2 for mantle earthquakes Mw>4 and ~0.4 for Mw<4, challenging the brittle failure assumption. Increased pore fluid pressure has been shown to lower stress ratios, implying that dehydration embrittlement may contribute to generating intermediate-depth seismicity in the Vrancea slab. Comparisons with seismic tomography and anisotropy studies show excellent correlations between maximum horizontal stress directions, possible slab strike orientation, and seismic anisotropy, especially below ~130 km depth, suggesting ambient mantle flow may also promote in-slab stress build-up and seismic potential.

## 1. Introduction

Intermediate-depth earthquake nests are isolated volumes of concentrated subcrustal seismicity (usually at the depths of 60–300 km) that are distinct from aftershock sequences or earthquake swarms due to their persistent seismic activity in time and unusual spatial isolation (e.g. Zarifi and Havskov, 2003). Earthquake nests are anomalous clusters because they are not necessarily located in or related to classic oceanic subduction systems at active plate margins. Three remarkable nests in the world are located in Bucaramanga (Colombia), Hindu Kush (Afghanistan), and Vrancea (Romania) (e.g. Prieto et al., 2012). The Vrancea seismic nest is a vertical cluster of intermediate-depth earthquakes located at the bend of the South-Eastern Carpathian Mountains in Europe (Fig. 1), where oceanic or continental subduction ended by 8–9 Ma, being followed by crustal deformation associated with the deeper evolution of a sinking seismogenic mantle body (Ismail-Zadeh et al., 2012; Maţenco, 2017). Studying the tectonic regimes and stress patterns in Vrancea and other similar seismic nests provides insights into earthquake generation processes beneath apparently locked collisional boundaries (Ismail-Zadeh et al., 2000), far from active plate margins, and may provide constraints on the type of the seismogenic slab (e.g. Chen et al., 2004) as well as its relation with the ambient mantle deformation (e.g. Carminati and Petricca, 2010; Ismail-Zadeh et al., 2005a). In this paper, we provide insights into intermediate-depth

* Corresponding author.
*E-mail address:* laura.petrescu90@gmail.com (L. Petrescu).

https://doi.org/10.1016/j.tecto.2020.228688
Received 16 July 2020; Received in revised form 14 October 2020; Accepted 15 November 2020
Available online 24 November 2020

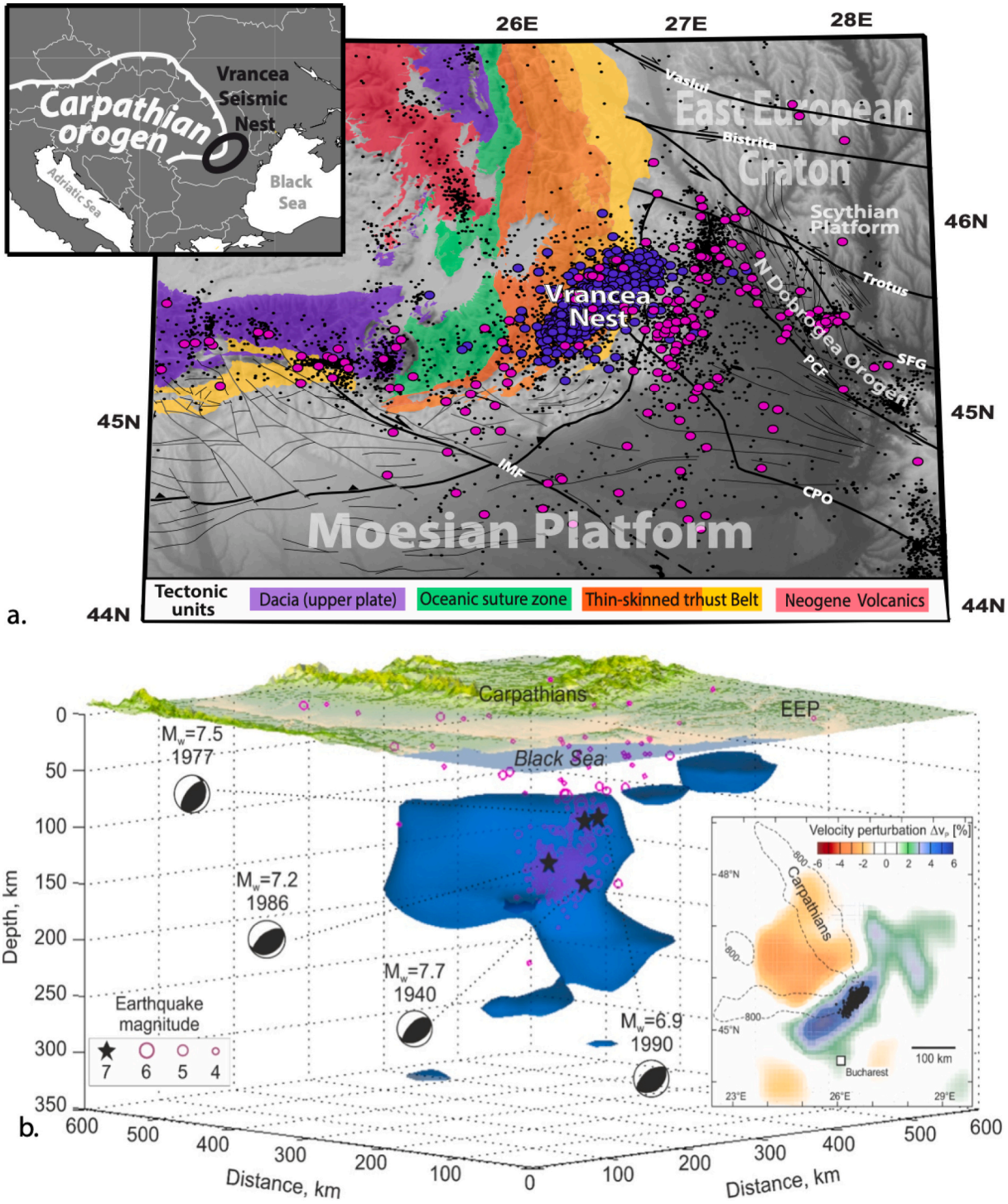


**Fig. 1.** a. Geologic and tectonic architecture of the South-East Carpathians and the foreland showing the major geological units in the Carpathians, the tectonic boundaries and major fault systems in the foreland, and regional seismicity in the crust (pink circles) and the upper mantle (dark circles) for which focal mechanisms were estimated and earthquakes without a mechanism solution (black dots). Fault name abbreviations are: CPO–Capidava-Ovidiu, PCF–Peceneaga-Camena, SFG–Sfantul Gheorghe, IMF–Intramoesian Fault. IMF is marked with a dashed line because it does not outcrop, being buried under Neogene sediments. Tectonic region abbreviations are: ND–North Dobrogea, SP–Scythian Platform. The upper left inset shows the location of the Vrancea seismic nest (black ellipse) in Central-Eastern Europe, at the bend of the SE Carpathian orogenic front (white line). b. Seismic-tomographic image of the Vrancea slab (Martin et al., 2006) and hypocenters of earthquakes (circles and asterisks indicate the location and magnitude of seismic events). The top surface illustrates the topography. The blue surface represents the isosurface of 3% positive anomalies of P-wave velocity obtained via teleseismic data inversion. Focal spheres are fault-plane solutions for the four largest Vrancea intermediate-depth earthquakes in the XXth century. The right panel presents the horizontal slice of the seismic-tomographic image at depth 100 km. (For interpretation of the references to colour in this figure legend, the reader is referred to the web version of this article.)

earthquake generation processes by updating the existing dataset of local seismicity (Radulian et al., 2019) with new waveform-estimated earthquake mechanisms from the past six years using multi-point source inversion (Sokos and Zahradnik, 2008). Furthermore, we determine the 3D variation of principal stress axes and maximum horizontal stress within the crust and the seismogenic body, using stress inversion software (Martnez-Garzón et al., 2014) based on an unsupervised machine-learning clustering algorithm and cubic gridding of focal mechanisms. Our results provide new constraints on the tectonic regime of a possibly coupled crust-mantle system in an anomalous seismic region.

## 2. Seismotectonics of the Vrancea region

The deep part of the Vrancea earthquake nest is confined to a narrow $\sim 100\,km(height) \times 70 \times 30\,km$ volume in the upper mantle beneath the SE Carpathians (Fig. 1, Radulian et al., 2008) and releases the highest strain in continental Europe (Oncescu and Bonjer, 1997; Wenzel et al., *1999*). Despite its remote location from the most active European collisional boundaries, the Vrancea earthquakes pose a significant seismic risk for the densely populated regions of Romania and neighbouring countries (e.g. Ismail-Zadeh et al., 2007; Sokolov et al., 2009). Seismic tomographic images reveal positive anomalies of seismic wave velocities in the upper-mantle beneath the southeastern (SE) Carpathians and the foreland region extending to depths of ~400 km (Wortel and Spakman, 2000; Martin et al., 2006; Koulakov et al., 2010; Ren et al., *2012*; Zhu et al., 2015; Baron and Morelli, 2017). The seismogenic zone is located within the shallower part of this elongated mantle anomaly, with seismicity rates peaking in two distinct depth ranges: 80–110 km and 120–170 km (Trifu and Radulian, 1989), and decreasing between 40 and 80 km, a depth range often interpreted as a weak coupling zone between the slab and the crust (e.g. Ismail-Zadeh et al., 2005b; Heidbach et al., 2007).

The Carpathians foreland formed on the lower tectonic plate in the former subduction system and is made upB59 of a collage of Precambrian continental units, some with repeated Paleozoic-Mesozoic deformations at the margins of the East European Craton, such as the Scythian Platform, the Moesian Platform (Săndulescu, 1988; Visarion et al., 1988), or the Hercynian-Cimmerian North Dobrogea Orogen (Fig. 1, Saccani et al., 2004; Saintot et al., 2006). Several NW-SE trending crustal-scale tectonic faults separate these continental units (Fig. 1), many of them seismogenic with variable kinematics from high-angle reverse faults beneath the orogen, to strike-slip and normal faulting in its foreland (e.g. Maţenco et al., 2007; Bocin et al., 2009; Diaconescu, *2017*).

In the upper tectonic plate relative to the former subduction system, the intra-Carpathian domain is made up of two major mega-units amalgamated during Paleozoic-Mesozoic times, i.e. ALCAPA and Tisza-Dacia (Csontos and Vörös, 2004; Schmid et al., 2020), among which the latter is relevant for the Vrancea zone of the SE Carpathians (Fig. 1). The two tectonic plates converged during Cretaceous-Cainozoic times, including by large scale clockwise rotations of Tisza-Dacia, in response to the larger Africa-Europe convergence of the entire Mediterranean domain (e.g. Van Hinsbergen et al., 2020; Roban et al., 2020). The last stages of Carpathians subduction and continental collision peaked during the Miocene until 8–9 Ma, when the subduction system was locked at crustal levels (e.g. Jiricek, 1979; Săndulescu, 1988; Maţenco et al., 2016). The overall subduction was followed by large scale differential motions in the orogen and its foreland associated with limited amounts of shortening, a process restricted to the area of SE Carpathians and still active, thought to be related to the deep evolution of the Vrancea seismogenic body (Leever et al., 2006; Maţenco et al., 2007; Ismail-Zadeh et al., 2012).

The overall inherited evolution created the Vrancea seismic zone situated at the junction of multiple continental units, sometimes defined as plates or micro-plates (e.g. Rădulescu et al., 1976; Beşuţiu et al., *2017*, among others). These continental units have heterogeneous seismic properties and a variable rheology that influenced continental buildup (e.g. Lankreijer et al., 1997; Cloetingh et al., 2004; Petrescu et al., 2019) and created a subducted slab of oceanic (e.g. Sperner et al., 2001; Bokelmann and Rodler, 2014) or continental (Knapp et al., *2005*; Fillerup et al., 2010) origin. Several geodynamic models have been proposed to explain its origin, ranging from slab retreat and roll-back (Royden, 1993; Linzer, 1996), various types of delamination (Grbacea and Frisch, *1998*; Chalot-Prat and Girbacea, 2000; Knapp et al., *2005a*; Fillerup et al., 2010), slab-detachment (e.g. Sperner et al., 2001), detachment and delamination (Gvirtzman, 2002; Göğüş et al., 2016) to gravitational instability (Ismail-Zadeh et al., 2000, 2005a, 2005b; Lorinczi and Houseman, 2009). We further refer to Ismail-Zadeh et al. (2012) for a detailed review of geodynamic mechanisms.

Previous studies have shown that the state of stress inside subducting slabs and the overlying crust can provide significant insights into the type of present geodynamic processes at play in the upper mantle and their effect on the tectonic regimes within the plates involved in the collision (e.g. Sperner et al., 2001; Carminati and Petricca, 2010; Petricca and Carminati, 2016) and may explain the mechanisms of earthquake generation both inside the slab and the overlying crust (e.g. Ismail-Zadeh et al., 2000, 2005a, 2005b). Moreover, changes in ambient mantle flow may play a significant role in the seismogenic potential in the overlying plate, even more significant than gravitational potential energy variations or lithospheric heterogeneities (e.g. Faccenna and Becker, 2010; Becker et al., 2015). Hence, we also explore possible connections between ambient mantle flow patterns and earthquake mechanisms. In the Vrancea area, earthquake mechanisms reveal mostly vertical tension and horizontal compression with widespread directions, generally thought to be related to vertical elongation inside a hypothetical subducted slab (Heidbach et al., 2007). However, a trend of mostly NE-SW oriented fault planes with perpendicular NW-SE compression can be observed inside the seismogenic body and a possible transition from compression to extension at shallower depth levels (Radulian et al., *1996*; Radulian et al., 1999). In the overlying crust, seismicity is largely asymmetric (Popa et al., 2003), with most earthquakes occurring in the foreland and beneath the orogen in the SE Carpathians area located between the Trotus and Intramoesian Faults (Fig. 1). Tectonic regimes have been described as heterogeneous with no particular orientation, and the slab may be decoupled or weakly coupled (Heidbach et al., 2007; Müller et al., 2010), which would inhibit stress transfer to the crust (Sperner et al., 2001). The causative relationship between mantle and shallow events was investigated by some authors (e.g. Mitrofan et al., 2014) who showed that focal depths decrease towards the actively subsiding foreland basin (i.e. Focsani Basin, Fig. 1) in the near-surface continuation of the deep Vrancea slab, providing arguments in favour of possible attachment between the mantle slab and overlying crust (Lorinczi and Houseman, 2009).

## 3. Methods and data

### 3.1. New waveform-estimated moment tensor solutions

Earthquake source parameters data used in this study includes the REFMC catalogue comprising 193 focal mechanisms from the 1952–2012 period in our study area of the SE Carpathians (Radulian et al., 2019, and references therein), and a 2013 seismic swarm from a microseismic zone SE of Vrancea comprising 17 mechanisms (Craiu et al., *2017*). We update these data with a new set of 18 moment tensor solutions of earthquakes Mw>3.5 from the 2014–2020 time period (see Supplementary Materials), estimated with a full waveform inversion algorithm as implemented in the ISOLA program package (Sokos and Zahradnik, 2008). The algorithm uses the method of least-squares to estimate the moment tensor and a grid search of the centroid position and time assuming a single point-source and an a priori moment-rate time dependence. The inversion is performed in the time domain

while the Earth response is represented by Green's functions computed using 1-D velocity model and discrete wavenumber algorithm (Bouchon, 1981). The frequency interval selected for the waveform inversion depends on the velocity model resolution (for high-frequency) and the signal-to-noise ratio (for the low-frequency inversion limit). Considering the moment rate as a delta function, the high-frequency limit also depends on the corner frequency of the earthquake. We ran the inversion using the 1-D velocity model proposed by Koulakov et al. (2010) for the Vrancea area. The grid search of centroids was performed on a set of predefined trial focal depths, coordinates, and origin times. We then manually focus on narrower search intervals for a fixed epicentre position until a satisfactory solution is obtained.

While tools for estimating earthquake source parameters have been long standing, associated uncertainties are not standardised and are usually derived from deviations from a particular assumed model, which makes it difficult to objectively compare our results with previous solutions (Radulian et al., 2019). In this study, a number of complementary inversion metrics are used concurrently to determine the reliability and quality of the inversion solution (see Supplementary Material). These are the signal-to-noise ratio (SNR), variance reduction (VR), the

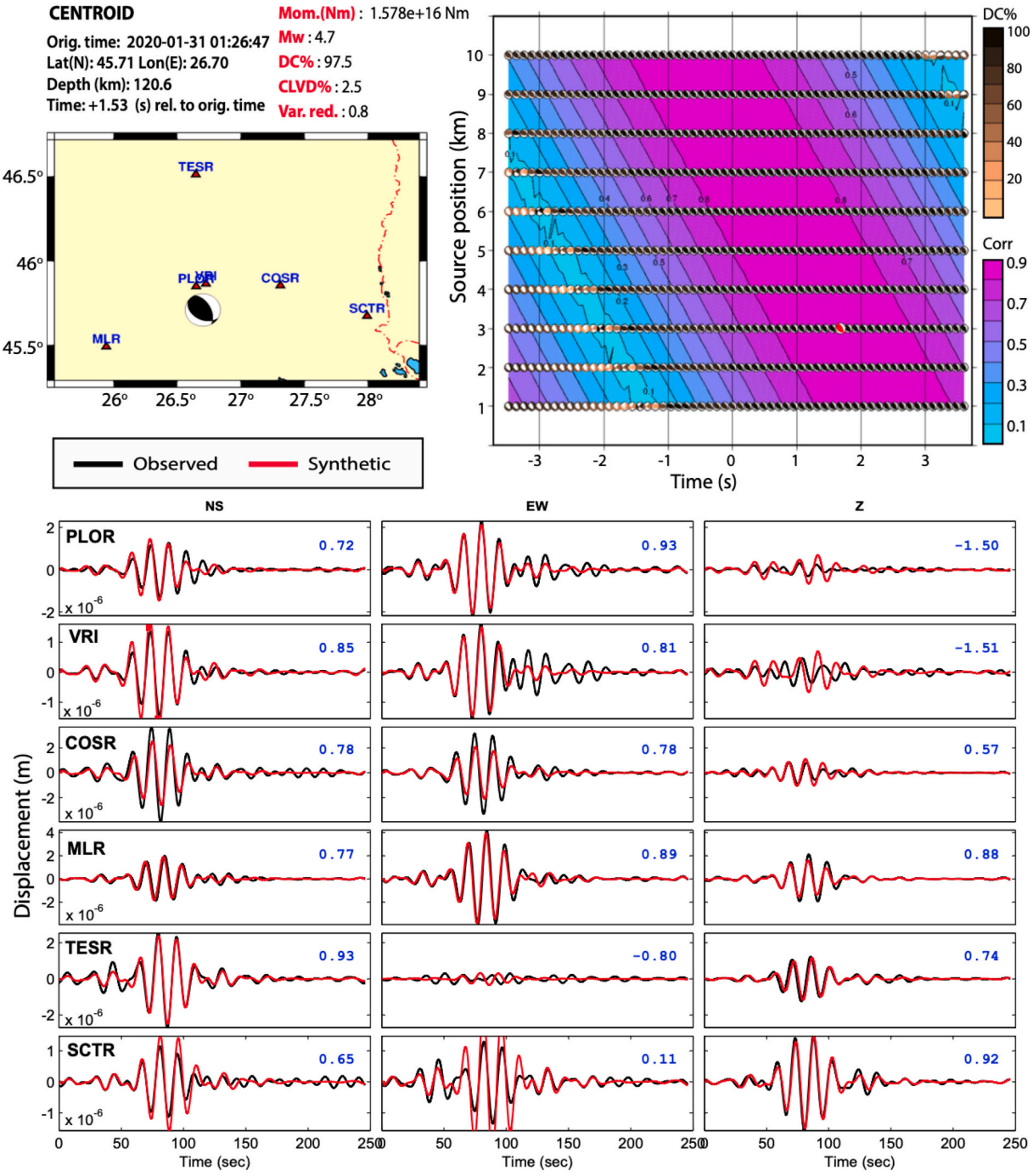


**Fig. 2.** Example of focal mechanism estimate with waveform inversion using the ISOLA code package (Sokos and Zahradnik, 2008). Top left: Focal mechanism solution information and map of earthquake epicentre and seismic stations used in the analysis. Top right: Cross-correlogram showing data fitness and trade-off between earthquake origin time and sources distributed between 108 km and 126 km depth, corresponding to the 1st and 10th source position, respectively. Bottom: Seismic waveforms used in the inversion and fitted synthetic waveforms corresponding to the inverted solution. Blue numbers are variance reduction values for each component. (For interpretation of the references to colour in this figure legend, the reader is referred to the web version of this article.)

condition number (a measurement of inversion reliability purely from a source-station configuration viewpoint), focal mechanisms variability index (the mean Kagan angle of all acceptable solutions for which the correlation between observed and synthetic waveforms is above 0.9), and the space-time variability index, measuring the area of acceptable solutions in the depth-origin time correlation plot, above the specified threshold (Sokos and Zahradnk, 2013). An example of a focal mechanism inversion solution from the Vrancea seismic nest estimated using local broadband seismic stations through the ISOLA package can be seen in Fig. 2.

To characterise the type of tectonic regimes present in the crust and the upper mantle, the type of faulting mechanism was determined using the software of Álvarez-Gómez (2019), which also includes oblique-slip regimes, based on the Johnston et al. *(1994)* classification. Ternary diagrams were produced with the Kaverina et al. (1996) projection, which is an improved version of the Frohlich (1992) method, for a range of

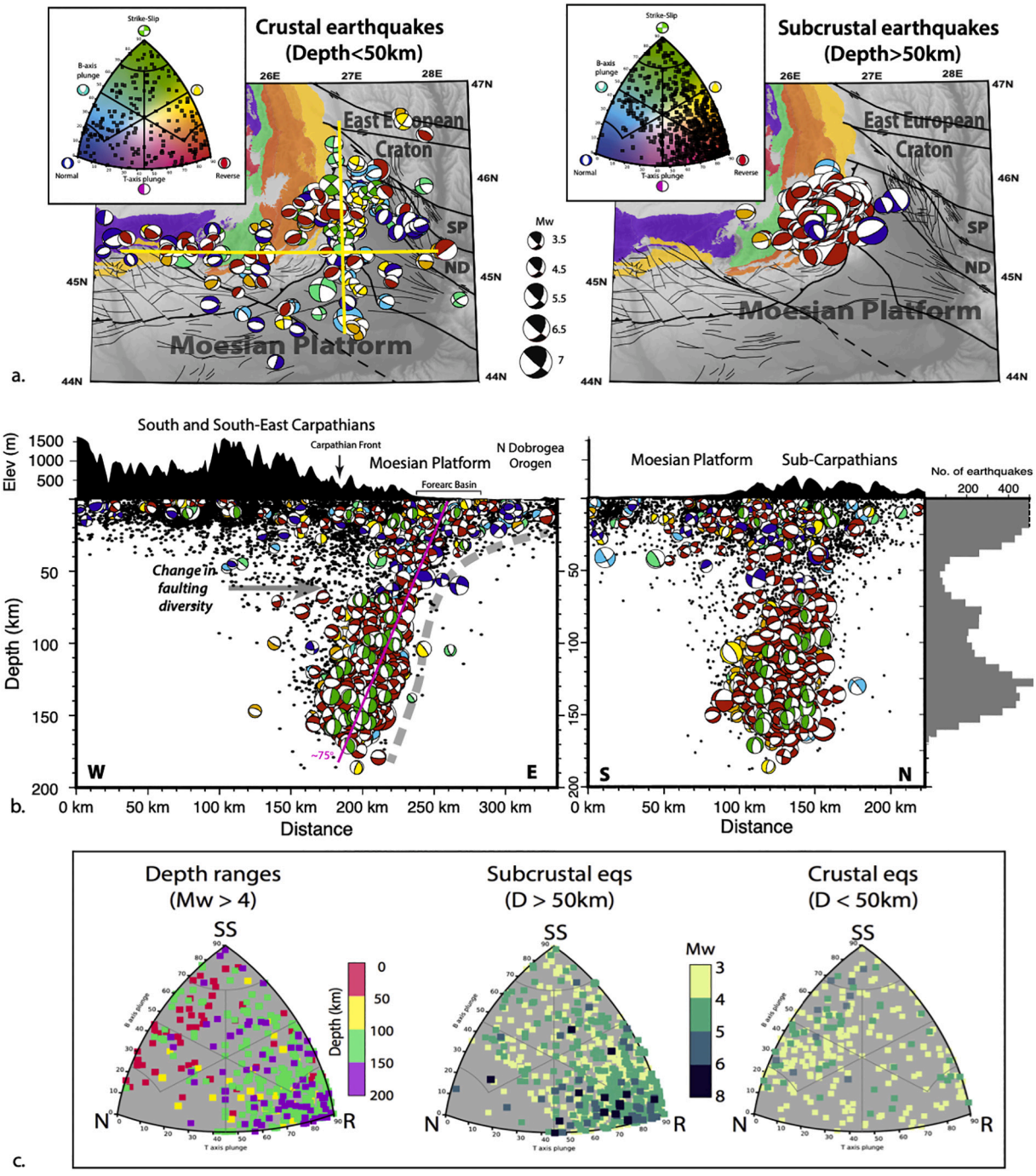


**Fig. 3.** a. Maps of the *V*rancea region showing earthquake mechanisms classified into seven types according to the values of the P, T and B centroid moment tensor axes (Álvarez-Gómez, 2019) with insets representing Kaverina diagrams (Kaverina et al., 1996). Earthquakes are represented in two depth ranges: 0–50 km (left map) and >50 km (right map). b. Cross-sections of seismicity (black dots) with focal mechanisms viewed from the south (left section) and from the east (right section). The topography is represented with black on top and locations of sections are marked as yellow lines in a. The right diagram is a histogram of earthquake number in 10 km depth bins. c. Kaverina diagrams of earthquake mechanisms of Mw>4 coloured with respect to their hypocentral depth (left diagram) and mechanisms coloured with respect to magnitude Mw occurring in the crustal (right) and upper mantle domain (centre), respectively. (For interpretation of the references to colour in this figure legend, the reader is referred to the web version of this article.)

hypocentral depths and magnitudes to probe whether secondary tectonic regimes appear in lower magnitude earthquakes or change with depth (Fig. 3c).

### 3.2. Earthquake data clustering

Focal mechanisms were first grouped into two main categories: those occurring within the crust, if their hypocentral depths were less than 50 km (approximated from 47 km, the maximum Moho depth in the SE Carpathians, Hauser et al., 2007; Diehl and Ritter, *2005*; Petrescu et al., 2019), and subcrustal earthquakes occurring below this depth (Fig. 3). The majority of crustal earthquakes is located in the foreland of the Carpathians, while the back-arc crustal region comprises local clusters of microearthquakes mostly located in volcanic structures (Fig. 1) for which there are no well-constrained focal mechanisms or moment tensor solutions available. The minimum and maximum geographic coordinates of the area likely influenced by the Vrancea slab dynamics were thus chosen between 24° – 29° in longitude (E) and 44° – 47° in latitude (N) ranges (Fig. 3). Subcrustal earthquakes are limited to an epicentral area of ~70 km×30 km and within a narrow upper-mantle

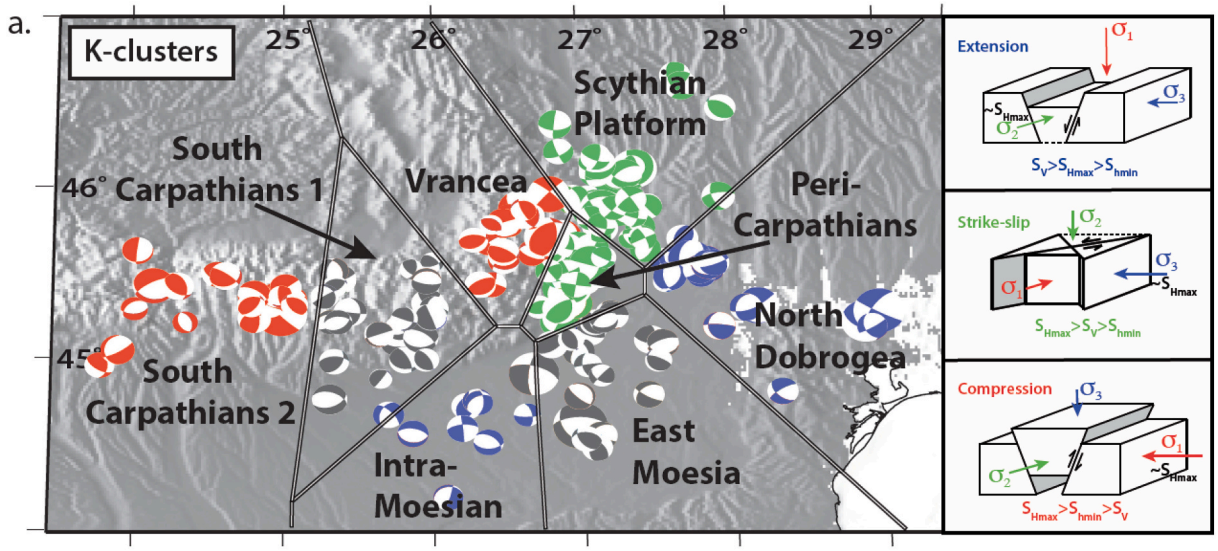


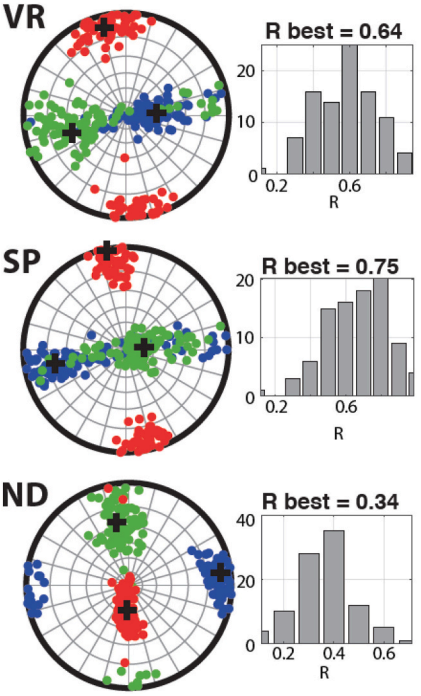


c.

| K-cluster | Horizontal axes | R value | Stress regime |
|---|---|---|---|
| Vrancea | $\sigma_1$,$\sigma_2$ | 0.64 | Compression |
| Scythian Platform | $\sigma_1$,$\sigma_3$ | 0.75 | Strike-slip |
| North Dobrogea | $\sigma_2$,$\sigma_3$ | 0.34 | Extension |
| East Moesian | n/a | 0.72 | Undefined |
| Intra-Moesian | $\sigma_2$,$\sigma_3$ | 0.25 | Extension |
| South Carpathians 1 | n/a | 0.72 | Undefined |
| South Carpathians 2 | $\sigma_1$,$\sigma_2$ | 0.61 | Compression |
| Peri-Carpathians | $\sigma_1$,$\sigma_3$ | 0.58 | Strike-slip |

**Fig. 4.** a. Crustal earthquake mechanisms clustered using the k-means partition algorithm. Lines are boundaries of the *V*oronoi cells generated by the algorithm for the considered area. Colours reflect the inversion solution for the dominant tectonic regime in each cluster: extensional (red), compressional (blue), strike-slip (green), and undefined (dark grey). Right inset: classification of tectonic regime, modified after Zoback and Zoback (2002). b. Examples of stress inversion results for selected clusters of focal mechanisms. These include stereonets showing the best-fit stress inversion solutions for the orientation of $\sigma_1$ (red), $\sigma_2$ (green), and $\sigma_3$ (blue) axes and their confidence intervals defined by the spread of the bootstrap resampling solutions (coloured dots). Each solution includes a histogram of the stress magnitude ratio value for each cluster. c. Table of stress regimes interpretations based on the directions of the principal axes and the value of the stress magnitude ratio, *R*. (For interpretation of the references to colour in this figure legend, the reader is referred to the web version of this article.)

volume extending to ~200 km depth (Fig. 3), so we chose a model grid with corner coordinates of 25.5° – 27.5° longitude (E) and 45° – 46.5° latitude (N).

The next step was to create a suitable model grid for the subsequent stress inversion and/or clustering of earthquakes based on their location, magnitude, depth, faulting regime, or association with a particular seismotectonic zone such as those classified by Bala et al. (2019). For crustal earthquakes, we used the unsupervised machine-learning k-means++ algorithm to cluster events based on their latitude-longitude coordinates. This is an iterative data partitioning technique that separates convex clusters by minimizing the average square distance between cluster points given pre-defined parameters such as a maximum number of clusters and or a maximum number of data points in each cluster (Lloyd, 1982; Arthur and Vassilvitskii, *2006*). We chose not to normalise coordinates prior to clustering, due to small feature variance and unit similarity. For our data, we found that the combination of input parameters of a maximum of k = 10 clusters with a minimum cluster size of 10 earthquakes, 200 iterations, and 5 random restarts yielded 8 stable regional clusters (Fig. 4) that are similar to previously classified seismotectonic zones (Bala et al., 2019). Increasing the number of maximum clusters did not affect the partitioning significantly due to the minimum forced cluster size. Although the number of iterations needed to ensure a convergence of k-means ranges from 20 to 50 (Broder et al., *2014*), we set this parameter to 200, to capture five random restarts, while also ensuring minimum convergence after each restart. The narrow subcrustal seismogenic domain (50–200 km) was optimally parameterised with a 3D cubic grid with latitude and longitude increments of 0.2° and 0.25°, respectively, and 30 km depth increments with a 20% overlap.

### 3.3. Stress inversion of focal mechanisms

Stress inversion was performed using the MSATSI software (Martnez-Garzón et al., *2014*) to find the best-fitted orientations of the principal stress axes of the reduced stress tensor ($\sigma_1 > \sigma_2 > \sigma_3$) and the stress magnitude ratio $R = \frac{\sigma_1 - \sigma_2}{\sigma_1 - \sigma_3}$ for each cluster/grid cell of focal mechanisms (see Supplementary Materials). We enforce a minimum of 10 earthquakes per grid cell (Fig. 4) to decrease the effect of outliers or focal mechanisms biased by potentially lower SNR. The R value is often overlooked and mostly used to assess the reliability of an inversion solution. Extremely low or high values of R imply either radial extension or radial compression, respectively, which in terms of strain suggest that deformation is related to either vertical elongation or vertical contraction. More recent research has shown that variations in the stress ratio correlate with injection rates in geothermal fields (Martnez-Garzón et al., *2016*), opening the possibility to investigate fluid pressure changes and deformation instability.

Like the majority of most stress inversion software, this method is based on the classical principle of conjugate faults and the Wallace-Bott criterion (Anderson, 1951; Wallace, 1951; Bott, 1959), which implies that slip on faults occurs in the direction of maximum resolved shear stress and is based on a number of assumptions, such as the slip direction must be parallel to the resolved shear stress direction, an isotropic medium, or the fault offset is negligible when compared with its dimensions. Although common in seismological research (e.g. Hardebeck and Hauksson, 2001; Kato et al., 2011; Martnez-Garzón et al., *2013*; Vavryčuk et al., 2015; Xu et al., 2016; Warren-Smith et al., 2019), fault mechanics and kinematic analysis have pointed out some weaknesses of such an approach, in particular when dealing with the uncertainties of resolving an incomplete stress tensor, reactivations, intersecting faults, large offset faults or shear zones, anisotropies or partitioning of strain in structures with different kinematics, such as observed in the SE Carpathians. Such limitations of the inversion methodology are otherwise well-discussed in fault-mechanics, paleostress and some geophysical studies (e.g. Orife and Lisle, 2003; Lund and Townend, 2007; Sperner and Zweigel, 2010; Célérier et al., 2012; Hippolyte et al., 2012). However, these types of inversions are useful to derive average stress solutions that are consistent with observed strain patterns in places where the crustal kinematics of the main faults are well-constrained (e.g. Simón, 2019, and references therein), such as the SE Carpathians.

Moment tensor solutions may be more heterogeneous in areas with a higher degree of strain partitioning, such as adjacent to large-offset faults or shear zones, but such effects are detected by kinematic and strain analysis, combined with GPS studies for active faults. A higher degree of confidence is given by coupling with the regional present-day stress derived from independent criteria (e.g. Heidbach et al., 2018). The quality of the stress inversion is assessed by estimating the 95% confidence region determined through a set of 500 bootstrap resamplings (Efron and Tibshirani, 1991) within each cluster of events. A damping parameter is also optimally defined during inversion based on the trade-off between model length and data misfit, which makes the solution more stable and uncertainties better constrained (Hardebeck and Michael, *2006*). Example of stress inversion results, bootstrap-defined confidence intervals and *R* histograms for selected crustal regions, as well as the tectonic regime significance for each *R*-$\sigma$ combination, are illustrated in Fig. 4. Further, the estimation of the direction of $S_{Hmax}$ represents another challenge. Often, it is calculated as the projection of the $\sigma$ that is closest to the horizontal, but this proxy can differ from the real $S_{Hmax}$ axis by as much as 24°. Here, we calculate the direction of $S_{Hmax}$ using a combination of $\sigma_1$, $\sigma_2$, and R, from the partial stress tensor solution in each cluster (Lund and Townend, 2007).

We specifically note that our inversion methodology was applied also to the Vrancea mantle earthquakes by assuming a brittle failure mechanism, an assumption far from obvious given the uncertain mechanics of intermediate-depth mantle earthquakes and alternative proposed hypotheses. These include mineralogical phase changes (e.g. Kirby et al., 1991), dehydration embrittlement (e.g. Ismail-Zadeh et al., 2000), or shear-heating and thermal runaway (e.g Kelemen and Hirth, 2007; John et al., 2009).

## 4. Results

### 4.1. Distribution of the updated focal mechanism data

Mantle earthquake focal mechanisms show a dominant thrust faulting regime with fault plane strikes scattered around a mean NE-SW direction (Fig. 3a), in agreement with previous studies (Oncescu and Trifu, 1987; Radulian et al., *2000*). Local occurrences of strike-slip, oblique-slip, and normal faulting are observed in the lower earthquake magnitude ranges (Fig. 3c). The distribution of earthquakes appears to outline a plane dipping at ~70° and three clusters of seismicity peaking in distinct depth ranges: 0–60 km, 80–110 km, and 120–170 km (Fig. 3b), similar to previous observations (Trifu and Radulian, 1989). At ~60 km depth, thrust faulting mechanisms show a transition to a volume with mixed focal mechanisms, ranging from thrusting to normal-faulting, and corresponds to a decrease in seismicity (Fig. 3b). This transition is visible on the depth-coloured earthquakes plotted on the Kaverina et al. (1996) diagram in Fig. 3c as well as on the W-E oriented cross-section in Fig. 3b. Radulian et al. *(1996)* suggested that there is a transition from compression to extension around this depth, but the improvement in data seems to point to a rather heterogeneous distribution at shallower levels. The longer recording period and improved station coverage during the past decade (Neagoe et al., *2019*) show that earthquakes occur at the depth interval of 40–60 km, previously considered a seismic gap (Hurukawa et al., 2008). Shallow seismicity (<50 km) is pervasive throughout the foreland and exhibits two different seismotectonic regimes depending on earthquake magnitude: Mw>5 earthquakes have a prevalent strike-slip and oblique-to-normal slip regime, while lower-magnitude events are more diverse (Fig. 3c). Hypocentral depths cluster and progressively increase beneath the foreland Focsani Basin, where pre-existing crustal structures such as

inferred rift-like features beneath the basin may play a role in localising seismicity (Panea et al., 2005; Tărăpoancă et al., 2004). Beneath the basin hypocenters appears to outline a bending plane on the SE side of the hypothetical slab interrupted by a few off-slab events (Fig. 3b). This is perhaps the strongest evidence in favour of coupling between the crustal and subcrustal seismogenic domains. Two seismicity peaks are evidenced in the intermediate depth range (Fig. 3b) but the transition between these two clusters is not marked by a change in focal mechanisms (Fig. 3c).

### 4.2. Stress patterns in the crust and upper mantle

The Vrancea cluster located above the seismogenic slab in the SE Carpathians bend zone is dominated by a compression regime with a N-S $\sigma_1$ (and $S_{Hmax}$) direction (Fig. 5a,b). A similar regime is estimated further west in the South Carpathians, with a NNE-SSW trending $\sigma_1$. The Peri-Carpathian cluster located in the foreland basin on the outer flanks of the SE Carpathians (Fig. 5b), overlying the slab bending region (Fig. 3b), shows a dominantly strike-slip regime with N-S trending $\sigma_1$, suggesting dextral (pure or changing to transpressive or transtensive) kinematics along the bended geometry of the Capidava-Ovidiu Fault, deeply buried in these locations at depths of up to 13 km (Fig. 5b). Another strike-slip dominated cluster is located NE of the Vrancea area at the intersection between multiple major faults (Fig. 5b). Here, $\sigma_1$ and $S_{Hmax}$ trend NNW-SSE, approximately parallel to the Peceneaga-Camena Fault close to its intersection with the Trotus Fault (Figs. 1, 5a,b). Further away from the Vrancea epicentral area in the foreland, stress regimes change to tension with dominantly N-S oriented $S_{Hmax}$ in North Dobrogea, and tension and transpression in the Moesian Platform, with NE-SW oriented $S_{Hmax}$ near the Intramoesian Fault (Fig. 5a,b). The transition from compression to strike-slip to tension thus appears to correlate with increasing distance from the Vrancea epicentral area, and is marked by regions of less well defined tectonic regimes, comprising oblique-slip mechanisms (trasn-tension or transpression).

The subcrustal seismogenic domain shows a more homogeneous stress pattern than the overlying crust, dominated by a systematically vertical and well-constrained $\sigma_3$ and horizontal $\sigma_1$, without a preferred orientation (Fig. 6). Vertical extension is thus predominant. However, the slab is not completely vertical (Fig. 3) and is thus at an angle with the extension direction and oblique to the maximum horizontal compression. The inversion for earthquakes with magnitudes Mw<4 versus those Mw>4 (see Supplementary Materials) shows a change in the stress ratio values between the two distributions (Fig. 6b,c): *R*-values for larger magnitude earthquakes are <0.3 (a prolate stress ellipsoid, $\sigma_1$ close to $\sigma_2$), while lower magnitude earthquakes *R*-values are as high as 0.7, increasing with decreasing depth, indicating a compressive regime.

Similar with $\sigma_1$, $S_{Hmax}$ orientations also vary within the slab at different depth levels (Fig. 7). Down to 120 km, directions display both NW-SE and NE-SW azimuths, with variable confidence angles and no particular correlation with either side of the elongated seismogenic body. In the ~120–150 km depth range, $S_{Hmax}$ directions are more coherently oriented NE-SW with better constrained confidence intervals towards the northwestern plane of the seismogenic body. Directions are less constrained towards the southeastern side. Below 150 km, seismicity becomes confined in a progressively narrower volume, but the NE-SW direction dominates across the slab.

## 5. Discussion

### 5.1. Stress relationships with past and present crustal deformation

The results of stress inversions of crustal earthquakes (Fig. 5a) are generally in agreement with the results of previous kinematic, structural, geophysical and geomorphological studies of the post-Miocene deformation (e.g. Necea et al., 2005; Fielitz and Seghedi, 2005; Leever et al., 2006; Maţenco et al., 2007; Bocin et al., 2009, and references therein), which showed a rapid change between reverse faulting in the orogen and the western part of the Focsani foreland basin, normal faulting along the eastern part of the Focsani basin and North Dobrogea unit, to strike-slip deformation limited to the transition zone between the SE Carpathians with the East and South Carpathians. These studies are consistent with our estimated stress field, ranging from compression in the SE Carpathian orogen and in the western part of the foredeep, to (trans)tension in the eastern part of the foredeep and North Dobrogea.

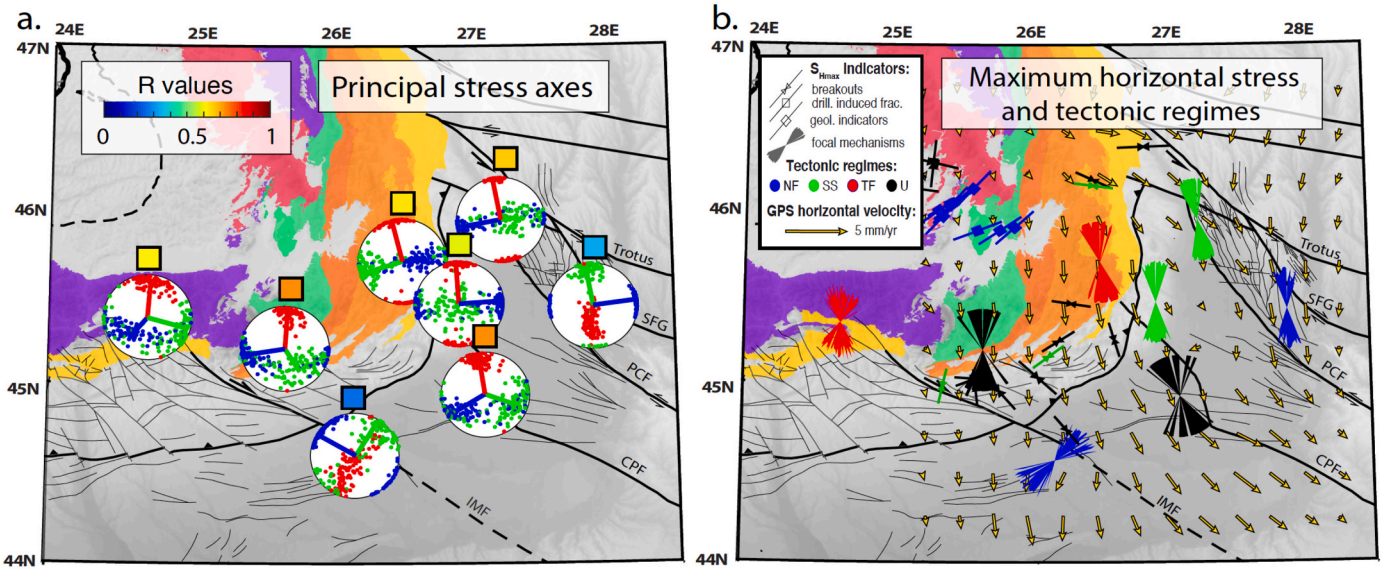


**Fig. 5.** a. Map of crustal stress inversion stereonets (white circles) containing principal stress axes ($\sigma_1$–red, $\sigma_2$–green, and $\sigma_3$–blue lines, respectively) and their bootstrap resampling solutions (coloured dots) estimated using MSATSI from crustal earthquake mechanisms clustered with the k-means algorithm. Stereonets are placed at the coordinates of each k-centroid. Relative stress magnitudes are also shown as coloured squares above each stereonet. b. Map of maximum horizontal stress ($S_{Hmax}$) orientations estimated from focal mechanism stress inversion solutions based on Lund and Townend (2007), coloured with respect to the tectonic regime. Other indicators for $S_{Hmax}$ include solutions from breakouts and geological indicators from the World Stress Map database generated using CASMO (Create a Stress Map Online, Heidbach et al., 2018). The yellow vector field represents the interpolated horizontal velocity vectors from geodetic measurements (Van der Hoeven et al., 2005). (For interpretation of the references to colour in this figure legend, the reader is referred to the web version of this article.)

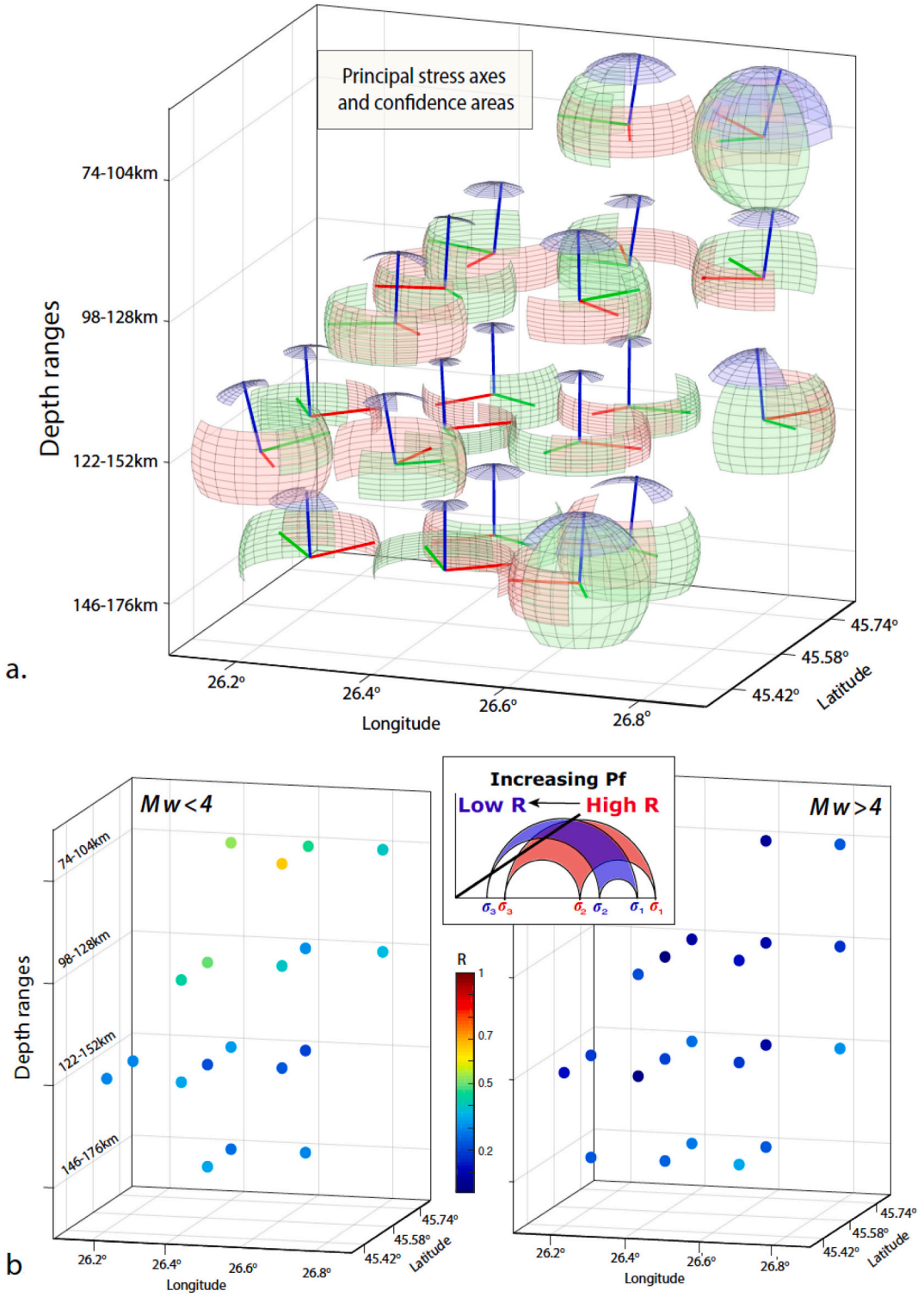


**Fig. 6.** a. Principal stress axes $\sigma_1$ (red), $\sigma_2$ (green), and $\sigma_3$ (blue) estimated using MSATSI from intermediate-depth Vrancea earthquakes, gathered in an overlapping 3D cubic grid model. Coloured regions represent areas of confidence for each axis, defined by the spread of the bootstrap resampling solutions. b. Relative stress magnitude values estimated after stress inversion of intermediate-depth earthquake mechanism clusters, for magnitudes Mw>4 (left) and Mw<4 (right). Inset shows Mohr circle diagrams for different relative stress magnitudes, showing the effect of increased pore fluid pressure (Pf). (For interpretation of the references to colour in this figure legend, the reader is referred to the web version of this article.)

The agreement between surface observations and deeper stress regime estimates based on earthquake focal mechanisms suggest that the stress field is vertically coherent on a crustal-scale, implying that similar deformation and seismogenic processes extend at mid-to-lower crustal depths. The margins of the deforming domain along the Trotus Fault and the northern part of the Peceneaga-Camena Fault (PCF), characterised mostly by a strike-slip stress field locally passing to transtension in the foreland (Fig. 5), are likely controlled by active crustal-scale movement along the PCF. The change from transtention to transpression towards or beneath the orogen correlates with an increased bending of the slab as

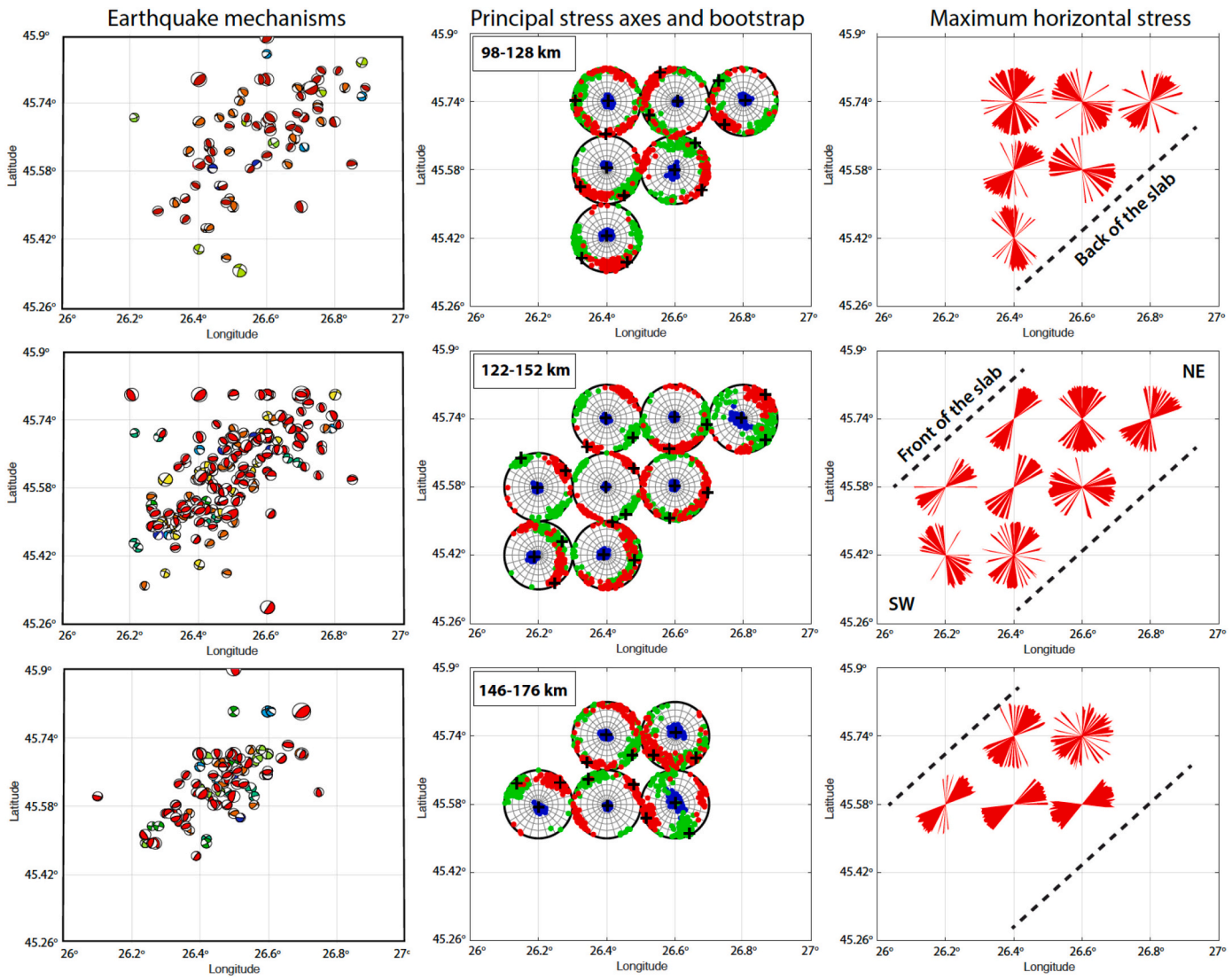


**Fig. 7.** Left: Depth slices of the best-fit principal stress axis solutions (crosses) inverted from the focal mechanism solutions of subcrustal earthquakes, and individual solutions from bootstrap analysis (coloured circles). Right: Maximum horizontal stress axes for each stress inversion solution.

outlined from seismicity (Fig. 3), suggesting that earthquakes here may be generated due to the slab bending (or unbending) forces acting in the shallower levels of the crust.

Present day horizontal and vertical movements in the Vrancea area have been estimated with GPS observations using temporary and permanent campaigns (Dinter et al., 2001; Van der Hoeven et al., 2005; Schmitt et al., *2007*). Vertical velocities show an alternating pattern of uplift and subsidence in the SE Carpathians, with ~10 mm/yr relative uplift rates (Van der Hoeven et al., 2005) or even as high as 22 mm/yr (Dinter et al., 2001). Uplift coincides with the location of the earthquake cluster where we obtained a compressive stress regime (Fig. 5b), with horizontal NNW-SSE oriented $\sigma_1$ axes and near-vertical $\sigma_3$. In the foreland basin and the majority of the eastern Moesian Platform, subsidence rates amount to ~10 mm/yr especially in the region between the IMF and PCF (Fig. 1), where the stress regime varies from strike-slip in the Peri-Carpathian cluster to dominantly tension farther away. In terms of strain, extension seems to be the main deformational effect ~100 km away from the Vrancea seismic nest. Active subsidence affected the foredeep since the 8–9 Ma and is probably still related to the negative buoyancy of the Vrancea slab (Ismail-Zadeh et al., 2005a, 2005b, 2012). Subsidence rates decrease towards the contacts with the Scythian and East European Platforms, where strike-slip is observed, switching to uplift in parts of the North Dobrogea Orogen (Van der Hoeven et al., 2005). The associated tension in the latter may indicate extension in the foredeep flexural bulge due to the high amount of cross-sectional bending of the lower tectonic plate (Fig. 3).

The horizontal velocity field reveals a movement towards the S-SE relative to Eurasia, of the entire SE Carpathian bend zone and its foreland, with rates on the order of 3 mm/yr or less (Van der Hoeven et al., 2005). Comparing the horizontal GPS-velocity field with our estimated $S_{Hmax}$ and previous stress measurements shows that the stress pattern closely correlates with the observed regional deformation (Fig. 5b). The post-9 Ma contraction recorded by large-scale folding of the foreland basin flanks and restricted to the SE Carpathians (Leever et al., 2006; Bocin et al., 2009) may have been transferred laterally to the foreland as transcurrent motion along the Trotus and Intramoesian faults (Fig. 1). This is consistent with the horizontal velocity measurements showing a large scale NNW-SSE movement that follows the curved trend of these faults and largely correlates with our estimated $S_{Hmax}$ orientations (Fig. 5), suggesting the present day stress-field may be evidence of ongoing compression distributed along the crustal-scale faults that mark the boundary between blocks of different mechanical strength. Nevertheless, this does not preclude a potential coupled slab scenario, if the magnitude of induced stresses outweighs the signature of the slab-pull.

### 5.2. Crust-mantle coupling versus second-order stress controls on crustal tectonics

The question "whether the Vrancea seismogenic mantle body (slab) is attached to the crust or not" is open. It has been suggested that the Vrancea slab is only partially coupled to the overlying crust (e.g. Heidbach et al., 2007) or that there is no coupling at all (e.g. Müller et al., 2010). Müller et al. (2010) modelled a cylindrical coupling region which resulted in a circular pattern of $S_{Hmax}$ distributions in the crust, contrary to observations (Fig. 5), from which the only conclusion possible was that the slab is only weakly or not coupled at all. Nevertheless, coupling scenarios often follow a simple geometry and do not always take into account the variable mechanical strength of the lithospheric blocks that make up the foreland (e.g. Lankreijer et al., 1997; Cloetingh et al., 2004). Our new results on stress patterns provide insights into the (de)coupling process, especially when checked against more complex numerical models. Geodynamic scenarios of delamination and break-off (Göğüş et al., 2016), weakly coupled (Fig. 8a,b) and already decoupled (Fig. 8c,d) slab (Ismail-Zadeh et al., 2005b) show that the modelled stress pattern in the slab and in the crust above it and those

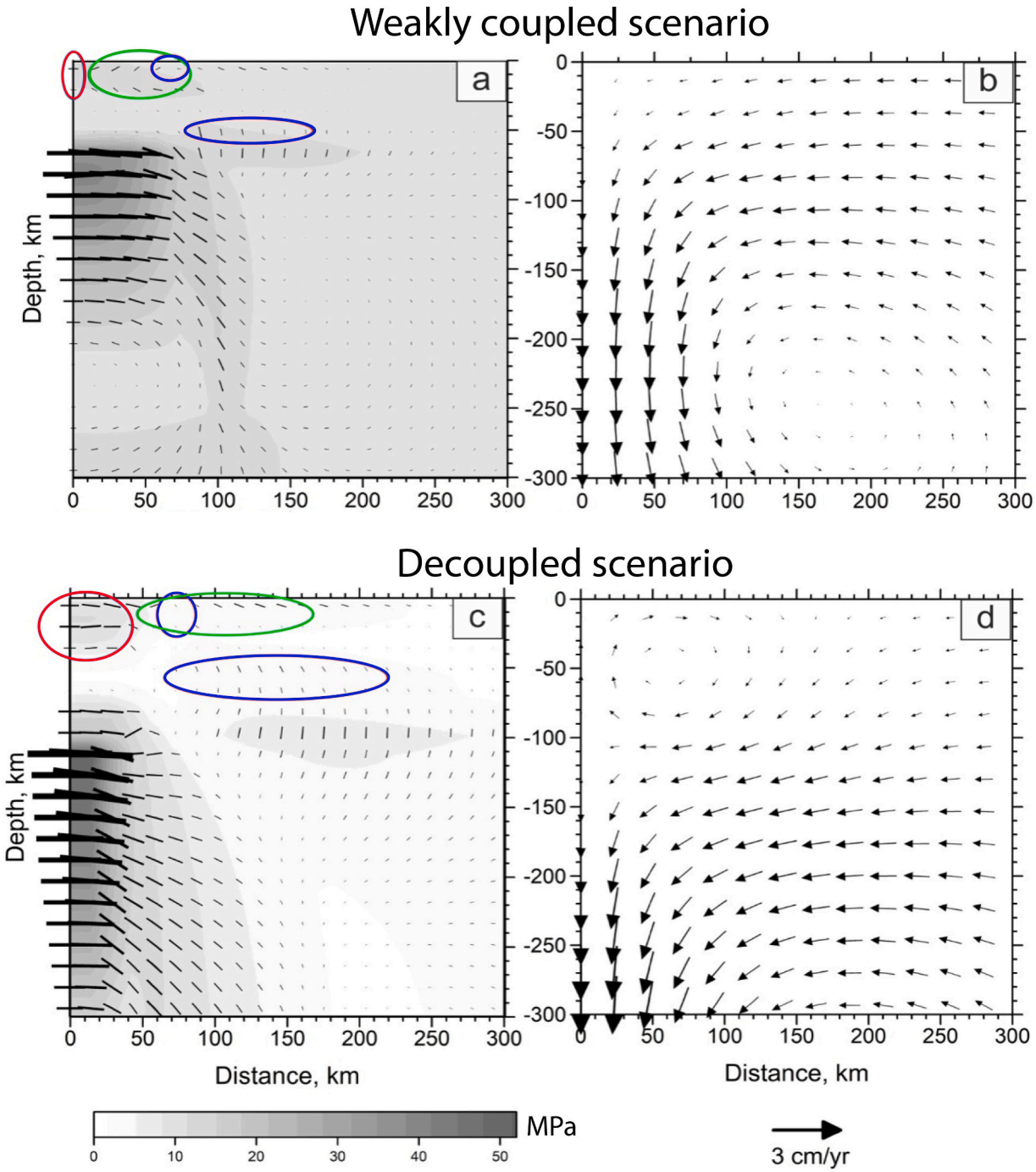


**Fig. 8.** Maximum tectonic shear stresses and axes of compression (left panels) and flow field (right panels) for the model of sinking Vrancea slab in the case of weak coupling between the slab and the crust (a, b) and decoupling (c,d). Coloured ellipses present the dominant stress regime: compression (red), strike-slip, transtension or transpression (green), and tension (blue). Modified after Ismail-Zadeh et al. (2005b). (For interpretation of the references to colour in this figure legend, the reader is referred to the web version of this article.)

obtained in this work have similarity. Namely, the tectonic stresses are predominantly compressional in the slab, and strike-slip faulting surrounding the body (compare to Figs. 3b, 6a). The decoupled model (Fig. 8c) shows a cluster of crustal compressional stresses just above the sinking body, also consistent with crustal shortening and thickening predicted above the presumed delaminating hinge, at the periphery of the hanging slab (Göğüş et al., 2016). Stress patterns indicate a change to predominantly strike-slip with some tensional components when moving further from Vrancea (compare to Fig. 5). Modelled normal stresses dominate at the depths of about 50–60 km (and down to ~140 km) at some distance from Vrancea. Similarly, our study obtained a dominantly tensional stress field beneath the Moesian Platform and North Dobrogea (see Figs. 3 and 5). The crustal stress patterns could be seen already on a smaller scale in the weakly coupled model (Fig. 8a) and are likely indicative of crust-slab decoupling initiation and rearrangement of mantle/crustal flow (Fig. 8b,d). Meanwhile our estimated orientations of principal stress axes (Fig. 6) are also compatible with the stress field induced by temperature contrasts in the upper mantle (Manea and Manea, 2009). In the latter model, the estimated maximum shear stress value can be as high as 200 MPa (Manea and Manea, 2009), while the detaching slab scenario predicts shear stress values of ~10 MPa in the crust and ~50 MPa in the 80–150 km depth range (Ismail-Zadeh et al., 2005b). This discrepancy raises the question whether temperature variations play a more important role in generating stress and whether formal stress inversions alone are able to discriminate between different mechanisms.

Second order stress controls in the crustal domain may include gravity potential of regional topography (e.g. Xu et al., 2016), stress reorientation at fault tips (e.g. Saucier et al., 1992), lithospheric heterogeneities (e.g. Zhan et al., 2016), or contrasting mechanical strength or density between adjacent blocks (Maţenco et al., 2007). The kinematics of the Trotus Fault and its various branches are thought to record the interaction between the northern segment of the East European Craton which underplates the East Carpathians, and a locked foreland segment to the south (Cloetingh et al., 2004). To the southeast, the PCF is documented to record foreland bulge uplift at the maximum Carpathian curvature due to increasing slab dip through time (Tărăpoancă et al., 2004; Cloetingh et al., 2004) or perhaps due to the migration of the delaminating hinge (Göğüş et al., 2016), although bending-related stresses may have decayed already since the Late Miocene when the Vrancea slab supposedly steepened (Müller et al., 2010). The estimated NNW-SSE trending $S_{Hmax}$ patterns obtained from earthquake mechanisms at the Trotus-PCF intersection show a dominantly strike-slip regime (although with large stress magnitude ratio uncertainty) that turns into extension further away along the North Dobrogea Orogen (Figs. 4,5). These patterns are consistent with models where both coupled slab dynamics and mechanical strength heterogeneities contribute to the observed foreland deformation (Cloetingh et al., 2004; Maţenco et al., 2007).

### 5.3. Slab stretching and possible dehydration embrittlement

From our results, one of the possible interpretations is that vertical elongation (in terms of strain) of the slab is driving the potential brittle failure and is the main mechanism affecting the orientation of the inferred stress field, where the direction of $\sigma_3$ is aligned along a slab geometry that is not completely vertical (Fig. 6), but horizontal shortening does not have a preferential orientation.Local 3D models of contemporary mantle flow and tectonic stress in the SE Carpathians (Ismail-Zadeh et al., 2005a, 2007) show that the dense slab or mantle drip sinking gravitationally beneath the Vrancea region (as imaged by Martin et al., *2001*, Martin et al., 2006) induces mantle downwelling and associated upwelling, but the slab dynamics could be complicated at intermediate-depths by toroidal (in horizontal planes) and poloidal (in vertical planes) flows. These patterns are consistent with a slab or another kind of lithospheric body that is gravitationally sinking and stretching (Ismail-Zadeh et al., 2005a, 2007), experiencing secondary deformational overprint possibly induced by more complex flow patterns or heterogeneous slab structure.

The mechanisms producing earthquakes at intermediate depths are still under debate, especially because at temperature-pressure conditions below 50 km rocks are expected to yield by creep or flow, so other mechanisms are required to enable brittle failure at such depths. Among the wide research available on the relationship between earthquakes and fluid flow dynamics (e.g. Snell et al., 2020, and references therein), the stress ratio has also been inferred to negatively correlate with changes in near-lithostatic pore fluid pressure for R<0.6 (Martnez-Garzón et al., *2016*). Specifically, the poroelastic response to increasing pore fluid pressure is larger in $\sigma_1$ and $\sigma_3$ than in $\sigma_2$ in an anisotropic medium such as fractured subducting slabs, thus lowering R (Healy, 2012; Warren-Smith et al., 2019). An increase in pore fluid pressure can arise from slab dehydration, enabling brittle failure at intermediate-depths. The change in stress ratio values from 0.3 to 0.7 for Mw>4 and Mw<4 earthquakes, respectively, suggest that small earthquakes are more clearly associated with preferential vertical elongation in the slab, while larger earthquakes could be generated by other mechanisms such as dehydration embrittlement.

### 5.4. Does mantle flow influence tectonic stresses?

Other 3D viscoelastic models taking into account external forces such as ambient mantle flow suggested that the angle between imposed flow and slab geometry can significantly contribute to the evolution of the stress field in the subducting lithosphere (e.g. Carminati and Petricca, 2010; Petricca and Carminati, 2016). One of the simulations included a slab that is concave and an ambient mantle flow direction opposing subduction (Petricca and Carminati, 2016). In this scenario, vertical tension and horizontal compression develop inside the slab (Petricca and Carminati, 2016), similar to the Vrancea observations (Figs. 6,7). Two sets of tensional axes are predicted by the models in this situation: those associated with the down-bending of the lithosphere in the shallow depth intervals, consistent with the vertical tension observed in the Vrancea epicentral area in the crust (Fig. 5), and those related to slab differential retreat due to mantle push affecting the intermediate levels. Down-dip tension and horizontal compression couples also rotate towards the slab edges (Petricca and Carminati, 2016), similar to the Vrancea patterns: $S_{Hmax}$ directions rotate from N-S and NW-SE in the shallower levels to dominantly NE-SW below ~130 km (Fig. 9).

Mantle flow is often inferred from seismic anisotropy studies such as SKS splitting (Ivan et al., 2008; Petrescu et al., 2020) or surface wave analysis (e.g. Zhu et al., 2015). Petrescu et al. (2020) detected large-scale NW-SE oriented flow below the Pannonian and Transylvanian Basins switching abruptly in the South and SE Carpathians, likely deviating along the edges of the thick lithosphere Moesian Plaform. Unlike previous seismic tomography studies, Ren et al. *(2012)* shows the Vrancea body connected to the SW with a wider positive anomaly extending beneath most of the Moesian Platform and the South Carpathians. The Vrancea nest lies at the northeastern tip of this seismic anomaly (Fig. 9) and is bounded by two seismically slow regions to the NW and SE. Mantle flow likely impacts the slab from the NW, switching to a NE-SW orientation (slab-parallel) in the SE Carpathians with localised asthenospheric upwelling on its front-side and N-S oriented flow behind it (Petrescu et al., 2020). In the shallower levels of the seismogenic body (80–130 km) $S_{Hmax}$ directions are more heterogeneous, displaying a mixture of NW-SE and NE-SW directions, without an obvious correlation with SKS fast anisotropy axes (Fig. 9). At deeper levels ($>130\,km$), however, $S_{Hmax}$ correlates well with the SKS directions estimated within the positive anomaly region and along its edges (Fig. 9). This correlation at depth is somewhat hard to explain since SKS splitting should, in theory, reflect the orientation of anisotropic a-type olivine crystals in the direction of maximum extension, while $S_{Hmax}$ is the direction of maximum horizontal compression. Preferential

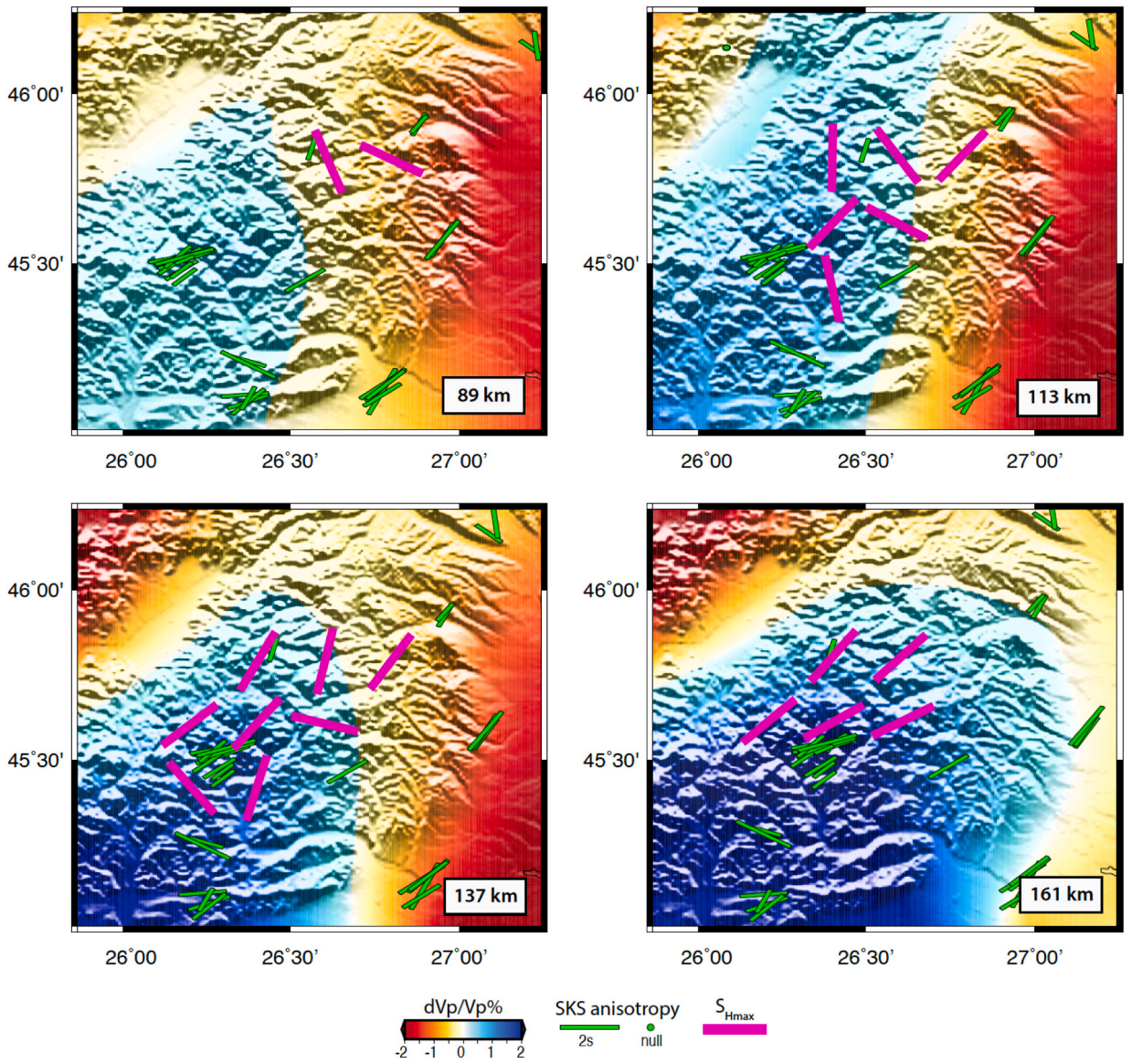


**Fig. 9.** Depth slices of P-wave tomography from Ren et al. *(2012)*, $S_{Hmax}$ estimated in this study (magenta lines), and SKS anisotropy fast directions (green bars) plotted at their piercing points at depths 89 km, 113 km, 137 km, and 161 km, respectively, from Petrescu et al. (2020). (For interpretation of the references to colour in this figure legend, the reader is referred to the web version of this article.)

alignment of fluid-filled cracks have been widely invoked to explain stress-aligned anisotropy especially in the crustal domains (e.g. Crampin and Lovell, 1991; Boness and Zoback, *2004*), although extending this hypothesis to the upper mantle is less likely. Nevertheless, the correlation between azimuthal anisotropy and maximum horizontal compression below 130 km is strong, opening the possibility for a physical connection between ambient mantle flow and earthquake generation in the descending lithospheric body.

### 5.5. Comparison with other seismic nests

The Hindu Kush nest, located in the eastern India-Asia collision zone in Afghanistan, has also been studied extensively (Prieto et al., 2012) and likely represents a zone of active delamination and roll-back (Kufner et al., 2016). When compared to Vrancea, earthquakes in the Hindu Kush extend deeper, down to ~280 km, and display a larger variation in tectonic regimes: no obvious preferred orientation is found at depths <180 km (Lister et al., 2008), but reverse-faulting dominates between 180 and 280 km. It has been suggested that Vrancea is an end-member of slab detachment (Sperner et al., 2001; Wortel and Spakman, 2000) and probably represents the fate of the Hindu Kush slab which might switch to a dominant vertical tension in the future, akin to the Vrancea dynamics. The Bucaramanga nest in Colombia comprises the highest concentration of intermediate-depth seismicity in the world (Zarifi and Havskov, 2003). Although P-T axes display significant scatter there (Cortés and Angelier, 2005), a slight tendency for SE-dipping tension may exist (Zarifi et al., 2007), suggesting the presence of a sinking slab that is breaking off similar to Vrancea. Some studies of seismic radiation patterns suggest earthquakes may also be generated via thermal shear instability in the Bucaramanga (Poli et al., 2016a) and Hindu Kush (Poli et al., 2016b) nests, especially in the detachment or "necking" region (Kufner et al., 2017). Vrancea earthquakes also exhibit depth-dependent clusters of seismicity and crust-mantle detachment most likely occurs in the 60–70 km range corresponding to reduced seismicity and a change in focal mechanism diversity (Fig. 3). However, more research into earthquake rupture processes is needed to probe thermal instability alternatives to earthquake nucleation in Vrancea. Local tectonic configurations may vary in these three unique intermediate-depth seismic zones

leading to a variation in stress within slabs. However, vertical extension seems to characterise each slab, albeit with different degrees of scattering, likely due to other factors such as regional mantle flow, slab origin, temperature and/or density heterogeneities.

## 6. Conclusions

The Vrancea Seismic Zone in Romania hosts a nest of intermediate-depth seismicity with frequent large magnitude earthquakes and is thought to represent an end-member of slab detachment where the subduction process was locked at crustal levels at 8 Ma. To investigate the tectonic regime and the geodynamic processes acting in the Vrancea area we estimated stress patterns through focal mechanism inversion. We updated the existing data with an extra 6 years of waveform-estimated earthquake source mechanisms and used an unsupervised machine-learning and cubic gridding to obtain seismic clusters in the crust and upper mantle, respectively. The present study brings arguments in favour of weak coupling (or an initiation of decoupling) between the sinking slab and the overriding crust, through seismicity distribution and stress regime patterns. The distribution of hypocenters show a progressive deepening towards the orogen, outlining a smooth bending of the SE side of the slab. Vertical tension and an overall compressive regime governs the stress field in the descending lithospheric body and seems to be transferred along the slab to the surface in the overlying crust, supporting a still coupled crust-mantle model where vertical elongation and down-bending are the driving mechanisms for brittle failure. We also identified a striking decrease in stress ratio (from 0.7 to 0.3) with increasing earthquake magnitudes (threshold Mw = 4), implying that small earthquakes are dominantly thrust-fault types associated with vertical elongation. This pattern speculatively suggests that other mechanisms such as mineralogical phase changes or dehydration embrittlement may potentially generate larger earthquakes at intermediate-depths. Our estimated stress patterns are also consistent with 3D viscoelastic stress models of a combination of slab-pull and mantle push (Petricca and Carminati, 2016), emphasising the seismogenic potential of ambient mantle flow. Comparisons with seismic tomography and anisotropy show excellent correlations between the average NE-SW slab strike, mantle deformation and maximum horizontal stress, especially below 120 km, suggesting that ambient mantle flow may be related to or promotes deformation within the slab, especially in its deeper levels.

In the crustal domain, maximum horizontal stress is mostly NNW-SSE oriented, in good agreement with the strike of most crustal faults in the foreland, and consistent with previous measurements of the horizontal velocity field as estimated with GPS observations which indicate a movement of the entire SE Carpathian bend zone and its foreland towards S-SE relative to Eurasia (Van der Hoeven et al., 2005). The stress regime changes to strike-slip, locally passing from transpression beneath the orogen to transtension in the foreland, and dominantly tensional further away, in the Moesian Platform and North Dobrogea Orogen. This pattern is consistent with results from previous geodynamic numerical models of a scenario where the slab is coupled to a crust composed of terrains with different rheological properties (e.g. Ismail-Zadeh et al., 2005b; Cloetingh et al., 2004). Our results thus provide enhanced insights into the origin of intermediate-depth earthquakes in a locked collisional setting, the deformation of a sinking detaching slab in its final stage and possible connections with ambient mantle flow, and suggests a causal connection with the tectonic regime distributions in the overlying crust.

## Declaration of Competing Interest

The authors declare that they have no known compe'ng financial interests or personal rela'onships that could have appeared to influence the work reported in this paper.

## Acknowledgments

LP is supported by the Romanian Ministry of Research and Innovation Research Grant NUCLEU–CIRRUS PN18150101/2018. Data for this analysis are freely available through the National Institute for Earth Physics upon request (www.infp.ro). We are grateful to Prof. Randell Stephenson, Piero Poli and an anonymous reviewer for critical and valuable comments that improved the manuscript. Most figures were made using GMT software (Wessel and Smith, 1998).

## Appendix A. Supplementary data

Supplementary data to this article can be found online at https://doi.org/10.1016/j.tecto.2020.228688.

## References

Álvarez-Gómez, J.A., 2019. FMC-Earthquake focal mechanisms data management, cluster and classification. SoftwareX 9, 299–307. https://doi.org/10.1016/j.softx.2019.03.008.

Anderson, E.M., 1951. The Dynamics of Faulting and Dyke Formation with Applications to Britain, 2nd edition. Oliver and Boyd, Edinburgh.

Arthur, D., Vassilvitskii, S., 2006. k-means++: the advantages of careful seeding, *Tech. rep.*, Stanford.

Bala, A., Toma-Danila, D., Radulian, M., 2019. Focal mechanisms in Romania: statistical features representative for earthquake-prone areas and spatial correlations with tectonic provinces. Acta Geod. Geophys. 54 (2), 263–286. https://doi.org/10.1007/s40328-019-00260-w.

Baron, J., Morelli, A., 2017. Full-waveform seismic tomography of the Vrancea, Romania, subduction region. Phys. Earth Planet. Inter. 273, 36–49. https://doi.org/10.1016/j.pepi.2017.10.009.

Becker, T.W., Lowry, A.R., Faccenna, C., Schmandt, B., Borsa, A., Yu, C., 2015. Western US intermountain seismicity caused by changes in upper mantle flow. Nature 524 (7566), 458–461. https://doi.org/10.1038/nature14867.

Beşuţiu, L., Manea, V., Pomeran, M., 2017. Vrancea seismic zone as an unstable triple junction: new evidence from observations and numerical modelling. In: 9th Congress of the Balkan Geophys. Soc, vol. 2017. European Association of Geoscientists & Engineers, pp. 1–5. https://doi.org/10.3997/2214-4609.201702541.

Bocin, A., Stephenson, R., Mocanu, V., Maţenco, L., 2009. Architecture of the South-Eastern Carpathians nappes and Focsani Basin (Romania) from 2D ray tracing of densely-spaced refraction data. Tectonophysics 476 (3–4), 512–527. https://doi.org/10.1016/j.tecto.2009.07.027.

Bokelmann, G., Rodler, F.-A., 2014. Nature of the Vrancea seismic zone (Eastern Carpathians)–New constraints from dispersion of first-arriving P-waves, *Earth Planet.* Sci. Lett. 390, 59–68. https://doi.org/10.1016/j.epsl.2013.12.034.

Boness, N.L., Zoback, M.D., 2004. Stress-induced seismic velocity anisotropy and physical properties in the SAFOD Pilot Hole in Parkfield, CA. Geophys. Res. Lett. 31 (15) https://doi.org/10.1029/2003GL019020.

Bott, M.H.P., 1959. The mechanics of oblique slip faulting. Geol. Mag. 96 (2), 109–117. https://doi.org/10.1017/S0016756800059987.

Bouchon, M., 1981. A simple method to calculate Green's functions for elastic layered media. Bull. Seismol. Soc. Am. 71 (4), 959–971.

Broder, A., Garcia-Pueyo, L., Josifovski, V., Vassilvitskii, S., Venkatesan, S., 2014. Scalable k-means by ranked retrieval, in *Proceedings of the 7th ACM international conference on Web search and data mining*, pp. 233–242.

Carminati, E., Petricca, P., 2010. State of stress in slabs as a function of large-scale plate kinematics. Geochem. Geophys. Geosyst. 11 (4).

Célérier, B., Etchecopar, A., Bergerat, F., Vergely, P., Arthaud, F., Laurent, P., 2012. Inferring stress from faulting: from early concepts to inverse methods. Tectonophysics 581, 206–219. https://doi.org/10.1016/j.tecto.2012.02.009.

Chalot-Prat, F., Girbacea, R., 2000. Partial delamination of continental mantle lithosphere, uplift-related crust–mantle decoupling, volcanism and basin formation: a new model for the Pliocene–Quaternary evolution of the southern East-Carpathians, Romania. Tectonophysics 327 (1–2), 83–107. https://doi.org/10.1016/S0040-1951(00)00155-4.

Chen, P.-F., Bina, C.R., Okal, E.A., 2004. A global survey of stress orientations in subducting slabs as revealed by intermediate-depth earthquakes. Geophys. J. Int. 159 (2), 721–733. https://doi.org/10.1111/j.1365-246X.2004.02450.x.

Cloetingh, S., Burov, E., Maţenco, L., Toussaint, G., Bertotti, G., Andriessen, P., Wortel, M., Spakman, W., 2004. Thermo-mechanical controls on the mode of continental collision in the SE Carpathians (Romania). Earth Planet. Sci. Lett. 218 (1–2), 57–76. https://doi.org/10.1016/S0012-821X(03)00645-9.

Cortés, M., Angelier, J., 2005. Current states of stress in the northern Andes as indicated by focal mechanisms of earthquakes. Tectonophysics 403 (1–4), 29–58. https://doi.org/10.1016/j.tecto.2005.03.020.

Craiu, A., Craiu, M., Diaconescu, M., Marmureanu, A., 2017. 2013 Seismic swarm recorded in Galati area, Romania: focal mechanism solutions. Acta Geod. Geophys. *52* (1), 53–67. https://doi.org/10.1007/s40328-016-0161-9.

Crampin, S., Lovell, J., 1991. A decade of shear-wave splitting in the Earth's crust: what does it mean? What can we make of it? And what should we do next? Geophys. J. Int. 107, 387–407.

Csontos, L., Vörös, A., 2004. Mesozoic plate tectonic reconstruction of the Carpathian region, *Palaeogeography, Palaeoclimatology*. Palaeoecology 210 (1), 1–56. https://doi.org/10.1016/j.palaeo.2004.02.033.
Diaconescu, M., 2017. Sisteme de fracturi active crustale pe teritoriul Romaniei, Ph.D. thesis, University of Bucharest, Romania.
Diehl, T., Ritter, J., C. group, 2005. The crustal structure beneath SE Romania from teleseismic receiver functions. Geophys. J. Int. 163 (1), 238–251. https://doi.org/10.1111/j.1365-246X.2005.02715.x.
Dinter, G., Nutto, M., Schmitt, G., Schmidt, U., Ghitau, D., Marcu, C., 2001. Three dimensional deformation analysis with respect to Plate Kinematic in Romania. Reports on Geodesy 2, 29–41.
Efron, B., Tibshirani, R., 1991. Statistical data analysis in the computer age. Science 253, 390–395.
Faccenna, C., Becker, T.W., 2010. Shaping mobile belts by small-scale convection. Nature 465 (7298), 602–605. https://doi.org/10.1038/nature09064.
Fielitz, W., Seghedi, I., 2005. Late Miocene–Quaternary volcanism, tectonics and drainage system evolution in the East Carpathians, Romania. Tectonophysics 410 (1–4), 111–136. https://doi.org/10.1016/j.tecto.2004.10.018.
Fillerup, M.A., Knapp, J.H., Knapp, C.C., Raileanu, V., 2010. Mantle earthquakes in the absence of subduction? Continental delamination in the Romanian Carpathians. Lithosphere 2 (5), 333–340. https://doi.org/10.1130/L102.1.
Frohlich, C., 1992. Triangle diagrams: ternary graphs to display similarity and diversity of earthquake focal mechanisms. Phys. Earth Planet. Inter. 75 (1–3), 193–198. https://doi.org/10.1016/0031-9201(92)90130-N.
Göğüş, O.H., Pysklywec, R.N., Faccenna, C., 2016. Postcollisional lithospheric evolution of the Southeast Carpathians: Comparison of geodynamical models and observations. Tectonics 35 (5), 1205–1224. https://doi.org/10.1002/2015TC004096.
Grbacea, R., Frisch, W., 1998. Slab in the wrong place: lower lithospheric mantle delamination in the last stage of the Eastern Carpathian subduction retreat. Geology 26 (7), 611–614. https://doi.org/10.1130/0091-7613(1998)026<0611:SITWPL>2.3.CO;2.
Gvirtzman, Z., 2002. Partial detachment of a lithospheric root under the Southeast Carpathians: toward a better definition of the detachment concept. Geology 30 (1), 51–54. https://doi.org/10.1130/0091-7613(2002)030<0051:PDOALR>2.0.CO;2.
Hardebeck, J.L., Hauksson, E., 2001. Crustal stress field in southern California and its implications for fault mechanics. J. Geophys. Res. 106 (B10), 21,859–21,882. https://doi.org/10.1029/2001JB000292.
Hardebeck, J.L., Michael, A.J., 2006. Damped regional-scale stress inversions: Methodology and examples for southern California and the Coalinga aftershock sequence. J. Geophys. Res. 111 (B11) https://doi.org/10.1029/2005JB004144.
Hauser, F., Raileanu, V., Fielitz, W., Dinu, C., Landes, M., Bala, A., Prodehl, C., 2007. Seismic crustal structure between the Transylvanian Basin and the Black Sea, Romania. Tectonophysics 430 (1–4), 1–25. https://doi.org/10.1016/j.tecto.2006.10.005.
Healy, D., 2012. Anisotropic poroelasticity and the response of faulted rock to changes in pore-fluid pressure, *Geological Society, London*. Special Publications 367 (1), 201–214. https://doi.org/10.1144/SP367.14.
Heidbach, O., Ledermann, P., Kurfeß, D., Peters, G., Buchmann, T., Matenco, L., Negut, M., Sperner, B., Müller, B., Nuckelt, A., et al., 2007. Attached or not attached: slab dynamics beneath Vrancea, Romania, in *Proceedings of the International Symposium on Strong Vrancea Earthquakes and Risk Mitigation, Bucharest, Romania*, 46, p. 320.
Heidbach, O., Rajabi, M., Cui, X., Fuchs, K., Müller, B., Reinecker, J., Reiter, K., Tingay, M., Wenzel, F., Xie, F., et al., 2018. The World stress Map database release 2016: Crustal stress pattern across scales. Tectonophysics 744, 484–498. https://doi.org/10.1016/j.tecto.2018.07.007.
Hippolyte, J.-C., Bergerat, F., Gordon, M.B., Bellier, O., Espurt, N., 2012. Keys and pitfalls in mesoscale fault analysis and paleostress reconstructions, the use of Angelier's methods. Tectonophysics 581, 144–162. https://doi.org/10.1016/j.tecto.2012.01.012.
Hurukawa, N., Popa, M., Radulian, M., 2008. Relocation of large intermediate-depth earthquakes in the Vrancea region, Romania, since 1934 and a seismic gap. Earth, Planets Space 60 (6), 565–572. https://doi.org/10.1186/BF03353119.
Ismail-Zadeh, A., Panza, G., Naimark, B., 2000. Stress in the descending relic slab beneath the Vrancea region. Romania. https://doi.org/10.1007/PL00001090.
Ismail-Zadeh, A., Mueller, B., Schubert, G., 2005a. Three-dimensional modeling of present-day tectonic stress beneath the earthquake-prone southeastern Carpathians based on integrated analysis of seismic, heat flow, and gravity observations. Phys. Earth Planet. Inter. 149 (1–2), 81–98. https://doi.org/10.1016/j.pepi.2004.08.012.
Ismail-Zadeh, A., Mueller, B., Wenzel, F., 2005b. Modelling of descending slab evolution beneath the SE-Carpathians: Implications for seismicity. In: Wenzel, F. (Ed.), *Perspectives in Modern Seismology, Lecture notes in Earth Sciences*, Vol. 205. Springer, Berlin, Heidelberg, pp. 203–223. https://doi.org/10.1007/978-3-540-31563-6-12.
Ismail-Zadeh, A., Sokolov, V., Bonjer, K.-P., 2007. Tectonic stress, seismicity, and seismic hazard in the southeastern Carpathians, *Nat.* Hazards 42 (3), 493–514. https://doi.org/10.1007/s11069-006-9074-1.
Ismail-Zadeh, A., Matenco, L., Radulian, M., Cloetingh, S., Panza, G., 2012. Geodynamics and intermediate-depth seismicity in Vrancea (the South-Eastern Carpathians): current state-of-the art. Tectonophysics 530, 50–79. https://doi.org/10.1016/j.tecto.2012.01.016.
Ivan, M., Popa, M., Ghica, D., 2008. SKS splitting observed at Romanian broad-band seismic network. Tectonophysics 462 (1–4), 89–98. https://doi.org/10.1016/j.tecto.2007.12.015.
Jiricek, R., 1979. Tectonic Development of the Carpathian Arc in the Oligocene and Neogene, *Tectonic Profiles Through the Western Carpathians*. Geological Institute Dionyz Stur, Bratislava, pp. 205–214.
John, T., Medvedev, S., Rüpke, L.H., Andersen, T.B., Podladchikov, Y.Y., Austrheim, H., 2009. Generation of intermediate-depth earthquakes by self-localizing thermal runaway. Nat. Geosci. 2 (2), 137–140. https://doi.org/10.1038/NGEO419.
Johnston, A., K. LR, C. KJ, Cornell, C.A., 1994. The earthquakes of stable continental regions. Volume 5: Seismicity database program and maps. Final report, vol. 5 (2519 pp).
Kato, A., Sakai, S., Iidaka, T., Iwasaki, T., Kurashimo, E., Igarashi, T., Hirata, N., Kanazawa, T., Katsumata, K., Takahashi, H., et al., 2011. Anomalous depth dependency of the stress field in the 2007 Noto Hanto, Japan, earthquake: potential involvement of a deep fluid reservoir. Geophys. Res. Lett. 38 (6) https://doi.org/10.1029/2010GL046413.
Kaverina, A., Lander, A., Prozorov, A., 1996. Global creepex distribution and its relation to earthquake-source geometry and tectonic origin. Geophys. J. Int. 125 (1), 249–265. https://doi.org/10.1111/j.1365-246X.1996.tb06549.x.
Kelemen, P.B., Hirth, G., 2007. A periodic shear-heating mechanism for intermediate-depth earthquakes in the mantle. Nature 446 (7137), 787–790. https://doi.org/10.1038/nature05717.
Kirby, S.H., Durham, W.B., Stern, L.A., 1991. Mantle phase changes and deep-earthquake faulting in subducting lithosphere. Science 252 (5003), 216–225. https://doi.org/10.1126/science.252.5003.216.
Knapp, J.H., Knapp, C.C., Raileanu, V., Matenco, L., Mocanu, V., Dinu, C., 2005. Crustal constraints on the origin of mantle seismicity in the Vrancea Zone, Romania: the case for active continental lithospheric delamination. Tectonophysics 410 (1), 311–323. https://doi.org/10.1016/j.tecto.2005.02.020.
Knapp, J., Asencio, E., Owens, T., Helffrich, G., 2005a. Integration of passive and active source seismology: Mapping lithospheric structure beneath Scotland, *AGU Fall Meeting Abstracts*, pp. A6+.
Koulakov, I., Zaharia, B., Enescu, B., Radulian, M., Popa, M., Parolai, S., Zschau, J., 2010. Delamination or slab detachment beneath Vrancea? New arguments from local earthquake tomography. Geochem. Geophys. Geosyst. 11 (3) https://doi.org/10.1029/2009GC002811.
Kufner, S.-K., Schurr, B., Sippl, C., Yuan, X., Ratschbacher, L., Ischuk, A., Murodkulov, S., Schneider, F., Mechie, J., Tilmann, F., et al., 2016. Deep India meets deep Asia: Lithospheric indentation, delamination and break-off under Pamir and Hindu Kush (Central Asia), *Earth Planet.* Sci. Lett. 435, 171–184. https://doi.org/10.1016/j.epsl.2015.11.046 0012-821X.
Kufner, S.-K., Schurr, B., Haberland, C., Zhang, Y., Saul, J., Ischuk, A., Oimahmadov, I., 2017. Zooming into the Hindu Kush slab break-off: a rare glimpse on the terminal stage of subduction, *Earth Planet.* Sci. Lett. 461, 127–140. https://doi.org/10.1016/j.epsl.2016.12.043.
Lankreijer, A., Mocanu, V., Cloetingh, S., 1997. Lateral variations in lithosphere strength in the Romanian Carpathians: constraints on basin evolution. Tectonophysics 272 (2–4), 269–290. https://doi.org/10.1016/S0040-1951(96)00262-4.
Leever, K., Matenco, L., Bertotti, G., Cloetingh, S., Drijkoningen, G., 2006. Late orogenic vertical movements in the Carpathian Bend Zone–seismic constraints on the transition zone from orogen to foredeep. Basin Res. 18 (4), 521–545. https://doi.org/10.1111/j.1365-2117.2006.00306.x.
Linzer, H.-G., 1996. Kinematics of retreating subduction along the Carpathian arc, Romania. Geology 24 (2), 167–170. https://doi.org/10.1130/0091-7613(1996)024<0167:KORSAT>2.3.CO;2.
Lister, G., Kennett, B., Richards, S., Forster, M., 2008. Boudinage of a stretching slablet implicated in earthquakes beneath the Hindu Kush. Nat. Geosci. 1 (3), 196–201. https://doi.org/10.1038/ngeo132.
Lloyd, S., 1982. Least squares quantization in PCM. IEEE Trans. Inf. Theory 28 (2), 129–137.
Lorinczi, P., Houseman, G., 2009. Lithospheric gravitational instability beneath the Southeast Carpathians. Tectonophysics 474 (1–2), 322–336. https://doi.org/10.1016/j.tecto.2008.05.024.
Lund, B., Townend, J., 2007. Calculating horizontal stress orientations with full or partial knowledge of the tectonic stress tensor. Geophys. J. Int. 170 (3), 1328–1335. https://doi.org/10.1111/j.1365-246X.2007.03468.xs.
Manea, V., Manea, M., 2009. Thermally induced stressed beneath the Vrancea area. In: Besutiu, L. (Ed.), Integrated Research on the Intermediate-Depth Earthquake Genesis within Vrancea Zone. Vergiliu, Bucharest, pp. 172–183.
Martin, M., Achauer, U., Kissling, E., Mocanu, V., Musacchio, G., Radulian, M., Wenzel, F., 2001. First results from the tomographic experiment CALIXTO99 in Romania, in *Geophys. Res. Abstr*, vol. 3.
Martin, M., Wenzel, F., C. W. Group, 2006. High-resolution teleseismic body wave tomography beneath SE-Romania-II. Imaging of a slab detachment scenario. Geophys. J. Int. 164 (3), 579–595. https://doi.org/10.1111/j.1365-246X.2006.02884.x.
Martnez-Garzón, P., Bohnhoff, M., Kwiatek, G., Dresen, G., 2013. Stress tensor changes related to fluid injection at the Geysers geothermal field, California, *Geophys.* Res. Lett. 40 (11), 2596–2601. https://doi.org/10.1002/grl.50438.
Martnez-Garzón, P., Kwiatek, G., Ickrath, M., Bohnhoff, M., 2014. MSATSI: a MATLAB package for stress inversion combining solid classic methodology, a new simplified user-handling, and a visualization tool. Seismol. Res. Lett. 85 (4), 896–904. https://doi.org/10.1785/0220130189.
Martnez-Garzón, P., Vavryčuk, V., Kwiatek, G., Bohnhoff, M., 2016. Sensitivity of stress inversion of focal mechanisms to pore pressure changes. Geophys. Res. Lett. 43 (16), 8441–8450. https://doi.org/10.1002/2016GL070145.
Matenco, L., 2017. Tectonics and exhumation of Romanian Carpathians: inferences from kinematic and thermochronological studies, in *Landform Dyn. and Ev. in Romania*, pp. 15–56, Springer.
Matenco, L., Bertotti, G., Leever, K., Cloetingh, S., Schmid, S.M., Tărăpoancă, M., Dinu, C., 2007. Large-scale deformation in a locked collisional boundary: Interplay

between subsidence and uplift, intraplate stress, and inherited lithospheric structure in the late stage of the SE Carpathians evolution. Tectonics 26 (4). https://doi.org/10.1029/2006TC001951.
Maţenco, L., Munteanu, I., Ter Borgh, M., Stanica, A., Tilita, M., Lericolais, G., Dinu, C., Oaie, G., 2016. The interplay between tectonics, sediment dynamics and gateways evolution in the Danube system from the pannonian basin to the western black sea. Sci. Total Environ. 543, 807–827.
Mitrofan, H., Chitea, F., Anghelache, M.-A., Visan, M., 2014. Possible Triggered Seismicity Signatures Associated with the Vrancea Intermediate-Depth strong Earthquakes (Southeast Carpathians, Romania). Seismol. Res. Lett. 85 (2), 314–323. https://doi.org/10.1785/0220130045.
Müller, B., Heidbach, O., Negut, M., Sperner, B., Buchmann, T., 2010. Attached or not attached-evidence from crustal stress observations for a weak coupling of the Vrancea slab in Romania. Tectonophysics 482 (1–4), 139–149. https://doi.org/10.1016/j.tecto.2009.08.022.
Neagoe, C., Manea, L.M., Marmureanu, A., Ionescu, C., 2019. A Review of Seismic Monitoring in Romania: improved earthquake detection network capabilities., in *Geophysical Research Abstracts*, vol. 21.
Necea, D., Fielitz, W., Matenco, L., 2005. Late Pliocene–Quaternary tectonics in the frontal part of the SE Carpathians: insights from tectonic geomorphology. Tectonophysics 410 (1–4), 137–156. https://doi.org/10.1016/j.tecto.2005.05.047.
Oncescu, M.-C., Bonjer, K.-P., 1997. A note on the depth recurrence and strain release of large Vrancea earthquakes. Tectonophysics 272 (2–4), 291–302. https://doi.org/10.1016/S0040-1951(96)00263-6.
Oncescu, M., Trifu, C.-I., 1987. Depth variation of moment tensor principal axes in Vrancea (Romania) seismic region. in *Annales geophysicae. Series B. Terrestrial and planetary physics* 5, 149–154.
Orife, T., Lisle, R.J., 2003. Numerical processing of palaeostress results. J. Struct. Geol. 25 (6), 949–957. https://doi.org/10.1016/S0191-8141(02)00120-7.
Panea, I., Stephenson, R., Knapp, C., Mocanu, V., Drijkoningen, G., Matenco, L., Knapp, J., Prodehl, K., 2005. Near-vertical seismic reflection image using a novel acquisition technique across the Vrancea Zone and Foscani Basin, South-Eastern Carpathians (Romania). Tectonophysics 410 (1–4), 293–309. https://doi.org/10.1016/j.tecto.2005.01.009.
Petrescu, L., Stuart, G., Tataru, D., Grecu, B., 2019. Crustal structure of the Carpathian Orogen in Romania from receiver functions and ambient noise tomography: how craton collision, subduction and detachment affect the crust. Geophys. J. Int. https://doi.org/10.1093/gji/ggz140.
Petrescu, L., Stuart, G., Houseman, G., Bastow, I., 2020. Upper mantle deformation signatures of craton-orogen interaction in the Carpathian-Pannonian region from SKS anisotropy analysis. Geophys. J. Int. https://doi.org/10.1093/gji/ggz573.
Petricca, P., Carminati, E., 2016. Present-day stress field in subduction zones: Insights from 3D viscoelastic models and data. Tectonophysics 667, 48–62. https://doi.org/10.1016/j.tecto.2015.11.010.
Poli, P., Prieto, G., Yu, C., Florez, M., Agurto-Detzel, H., Mikesell, T., Chen, G., Dionicio, V., Pedraza, P., 2016a. Complex rupture of the M 6.3 2015 March 10 Bucaramanga earthquake: evidence of strong weakening process. Geophys. J. Int. 205 (2), 988–994. https://doi.org/10.1093/gji/ggw065.
Poli, P., Prieto, G., Rivera, E., Ruiz, S., 2016b. Earthquakes initiation and thermal shear instability in the Hindu Kush intermediate depth nest. Geophys. Res. Lett. 43 (4), 1537–1542. https://doi.org/10.1002/2015GL067529.
Popa, M., Grecu, B., Popescu, E., Placinta, A., Radulian, M., 2003. Asymmetric distribution of seismic motion across the south-eastern Carpatians (Romania) and its implications. Rom. Rep. Phys. 55 (3), 521–534.
Prieto, G.A., Beroza, G.C., Barrett, S.A., López, G.A., Florez, M., 2012. Earthquake nests as natural laboratories for the study of intermediate-depth earthquake mechanics. Tectonophysics 570, 42–56. https://doi.org/10.1016/j.tecto.2012.07.019.
Rădulescu, D., Cornea, I., Sndulescu, M., Constantinescu, P., Rdulescu, F., Pompilian, A., 1976. Structure de la croûte terrestre en roumanie. essai d'interprétation des études séismiques profondes. Anuarul Institutului de Geologie şi Geofizica 50, 5–36.
Radulian, M., Mândrescu, N., Popescu, E., Utale, A., Panza, G., 1996. Seismic activity and stress field characteristics for the seismogenic zones of Romania, *ICTP Preprint IC/96/256*.
Radulian, M., Mandrescu, N., Popescu, E., Utale, A., Panza, G., 1999. Seismic activity and stress field in Romania. Romanian Journal of Physics 44 (9–10), 1051–1069.
Radulian, M., Mandrescu, N., Panza, G., Popescu, E., Utale, A., 2000. Characterization of seismogenic zones of Romania, in *Seismic Hazard of the Circum-Pannonian Region*. Springer, pp. 57–77.
Radulian, M., Popa, M., Cărbunar, O., Rogozea, M., 2008. Seismicity patterns in Vrancea and predictive features. Acta Geod. Geophys. Hung. 43 (2–3), 163–173.
Radulian, M., Bălă, A., Ardeleanu, L., Toma-Dănilă, D., Petrescu, L., Popescu, E., 2019. Revised catalogue of earthquake mechanisms for the events occurred in Romania until the end of twentieth century: REFMC. Acta Geod. Geophys. 54 (1), 3–18. https://doi.org/10.1007/s40328-018-0243-y.
Ren, Y., Stuart, G., Houseman, G., Dando, B., Ionescu, C., Hegedüs, E., Radovanović, S., Shen, Y., S. C. P. W. Group, et al., 2012. Upper mantle structures beneath the Carpathian–Pannonian region: Implications for the geodynamics of continental collision, *Earth Planet.* Sci. Lett. 349, 139–152. https://doi.org/10.1016/j.epsl.2012.06.037.
Roban, R., Ducea, M., Maenco, L., Panaiotu, G., Profeta, L., Krézsek, C., Melinte-Dobrinescu, M., Anastasiu, N., Dimofte, D., Apotrosoaei, V., et al., 2020. Lower cretaceous provenance and sedimentary deposition in the Eastern Carpathians: Inferences for the evolution of the subducted oceanic domain and its European passive continental margin, *Tectonics*, p. e2019TC005780. https://doi.org/10.1029/2019TC005780.
Royden, L.H., 1993. Evolution of retreating subduction boundaries formed during continental collision. Tectonics 12 (3), 629–638. https://doi.org/10.1029/92TC02641.
Saccani, E., Seghedi, A., Nicolae, I., 2004. Evidence of rift magmatism from preliminary petrological data on lower Triassic mafic rocks from the North Dobrogea orogen (Romania). Ofioliti 29 (2), 231–241.
Saintot, A., Stephenson, R.A., Stovba, S., Brunet, M.-F., Yegorova, T., Starostenko, V., 2006. The evolution of the southern margin of eastern europe (eastern european and scythian platforms) from the latest precambrian-early palaeozoic to the early cretaceous, *Geological Society, London*. Memoirs 32 (1), 481–505. https://doi.org/10.1144/GSL.MEM.2006.032.01.30.
Săndulescu, M., 1988. Cenozoic Tectonic history of the Carpathians. In: Royden, L.H., Horvaáth, F. (Eds.), The Pannonian Basin, a Study in Basin Evolution., Am. Assoc. Pet. Geol. Mem, 157, pp. 17–25.
Saucier, F., Humphreys, E., Weldon, R., 1992. Stress near geometrically complex strike-slip faults: Application to the San Andreas fault at Cajon Pass, southern California. J. Geophys. Res. 97 (B4), 5081–5094. https://doi.org/10.1029/91JB02644.
Schmid, S.M., Fügenschuh, B., Kounov, A., Maţenco, L., Nievergelt, P., Oberhänsli, R., Pleuger, J., Schefer, S., Schuster, R., Tomljenović, B., et al., 2020. Tectonic units of the Alpine collision zone between Eastern Alps and western Turkey. Gondwana Res. 78, 308–374. https://doi.org/10.1016/j.gr.2019.07.005.
Schmitt, G., Nuckelt, A., Knöpfler, A., Marcu, C., 2007. Three dimensional plate kinematics in Romania, in *Proc. Int. Symp. Strong Vrancea Earthquakes and Risk Mitigation*, pp. 34–45, Bucharest Romania.
Simón, J.L., 2019. Forty years of paleostress analysis: has it attained maturity? J. Struct. Geol. 125, 124–133. https://doi.org/10.1016/j.jsg.2018.02.011.
Snell, T., De Paola, N., van Hunen, J., Nielsen, S., Collettini, C., 2020. Modelling fluid flow in complex natural fault zones: Implications for natural and human-induced earthquake nucleation. *Earth Planet.* Sci. Lett. 530, 115,869. https://doi.org/10.1016/j.epsl.2019.115869.
Sokolov, V.Y., Wenzel, F., Mohindra, R., 2009. Probabilistic seismic hazard assessment for Romania and sensitivity analysis: a case of joint consideration of intermediate-depth (Vrancea) and shallow (crustal) seismicity. Soil Dyn. Earthq. Eng. 29 (2), 364–381. https://doi.org/10.1016/j.soildyn.2008.04.004.
Sokos, E.N., Zahradnik, J., 2008. ISOLA a Fortran code and a Matlab GUI to perform multiple-point source inversion of seismic data. Comput. Geosci. 34 (8), 967–977. https://doi.org/10.1016/j.cageo.2007.07.005.
Sokos, E., Zahradnk, J., 2013. Evaluating centroid-moment-tensor uncertainty in the new version of ISOLA software. Seismol. Res. Lett. 84 (4), 656–665. https://doi.org/10.1785/0220130002.
Sperner, B., Zweigel, P., 2010. A plea for more caution in fault–slip analysis. Tectonophysics 482 (1–4), 29–41. https://doi.org/10.1016/j.tecto.2009.07.019.
Sperner, B., Lorenz, F., Bonjer, K., Hettel, S., Müller, B., Wenzel, F., 2001. Slab break-off–abrupt cut or gradual detachment? New insights from the Vrancea Region (SE Carpathians, Romania). Terra Nova 13 (3), 172–179. https://doi.org/10.1046/j.1365-3121.2001.00335.x.
Tărăpoancă, M., Garcia-Castellanos, D., Bertotti, G., Matenco, L., Cloetingh, S., Dinu, C., 2004. Role of the 3-D distributions of load and lithospheric strength in orogenic arcs: polystage subsidence in the Carpathians foredeep. Earth Planet. Sci. Lett. 221 (1–4), 163–180. https://doi.org/10.1016/S0012-821X(04)00068-8.
Trifu, C.-I., Radulian, M., 1989. Asperity distribution and percolation as fundamentals of an earthquake cycle. Phys. Earth Planet. Inter. 58 (4), 277–288. https://doi.org/10.1016/0031-9201(89)90100-3.
Van der Hoeven, A., Mocanu, V., Spakman, W., Nutto, M., Nuckelt, A., Maţenco, L., Munteanu, L., Marcu, C., Ambrosius, B., 2005. Observation of present-day tectonic motions in the Southeastern Carpathians: results of the ISES/CRC-461 GPS measurements. Earth Planet. Sci. Lett. 239 (3–4), 177–184. https://doi.org/10.1016/j.epsl.2005.09.018.
Van Hinsbergen, D.J., Torsvik, T.H., Schmid, S.M., Maţenco, L.C., Maffione, M., Vissers, R.L., Gürer, D., Spakman, W., 2020. Orogenic architecture of the Mediterranean region and kinematic reconstruction of its tectonic evolution since the Triassic. Gondwana Res. 81, 79–229. https://doi.org/10.1016/j.gr.2019.07.009.
Vavryčuk, V., Beer, M., Kougioumtzoglou, I., Patelli, E., Au, I., 2015. Earthquake mechanisms and stress field, *Encyclopedia of earthquake engineering*, pp. 728–746.
Visarion, M., Sandulescu, M., Stanica, D., Veliciu, S., 1988. Contributions a la connaissance de la structure profonde de la plateforme Moesienne en Roumanie, *St.* Tehn. Econ., Ser. Geogiz., D, 15, pp. 211–222.
Wallace, R.E., 1951. Geometry of shearing stress and relation to faulting. J. Geol. 59 (2), 118–130. https://doi.org/10.1086/625831.
Warren-Smith, E., Fry, B., Wallace, L., Chon, E., Henrys, S., Sheehan, A., Mochizuki, K., Schwartz, S., Webb, S., Lebedev, S., 2019. Episodic stress and fluid pressure cycling in subducting oceanic crust during slow slip. Nat. Geosci. 12 (6), 475–481.
Wenzel, F., Lorenz, F., Sperner, B., Oncescu, M., 1999. Seismotectonics of the Romanian Vrancea area, in *Vrancea Earthquakes: Tectonics, Hazard and Risk Mitigation*. Springer, pp. 15–25.
Wessel, P., Smith, W.H., 1998. New, improved version of Generic Mapping Tools released, *Eos.* Trans. Am. Geophys. Union 79 (47), 579.
Wortel, M., Spakman, W., 2000. Subduction and slab detachment in the Mediterranean-Carpathian region. Science 290 (5498), 1910–1917. https://doi.org/10.1126/science.290.5498.1910.
Xu, Z., Huang, Z., Wang, L., Xu, M., Ding, Z., Wang, P., Mi, N., Yu, D., Li, H., 2016. Crustal stress field in Yunnan: implication for crust-mantle coupling. Earthq. Sci. 29 (2), 105–115. https://doi.org/10.1007/s11589-016-0146-3.
Zarifi, Z., Havskov, J., 2003. Characteristics of dense nests of deep and intermediate-depth seismicity. Adv. Geophys. 46, 238–278.

Zarifi, Z., Havskov, J., Hanyga, A., 2007. An insight into the Bucaramanga nest. Tectonophysics 443 (1–2), 93–105. https://doi.org/10.1016/j.tecto.2007.06.004.
Zhan, Y., Hou, G., Kusky, T., Gregg, P.M., 2016. Stress development in heterogenetic lithosphere: Insights into earthquake processes in the New Madrid Seismic Zone. Tectonophysics 671, 56–62. https://doi.org/10.1016/j.tecto.2016.01.016.
Zhu, H., Bozdağ, E., Tromp, J., 2015. Seismic structure of the European upper mantle based on adjoint tomography. Geophys. J. Int. 201 (1), 18–52. https://doi.org/10.1093/gji/ggu492.
Zoback, M.D., Zoback, M.L., 2002. Stress in the Earths lithosphere. Encyclopedia Physical Sci. Technol. 16, 143–154.